Journal of Asian Earth Sciences xxx (xxxx) 106086

Contents lists available at ScienceDirect

Journal of Asian Earth Sciences

journal homepage: www.elsevier.com/locate/jseaes

Full length article

Multi-stages of Paleozoic deformation of the fault system in the Tazhong Uplift, Tarim Basin, NW China: Implications for hydrocarbon accumulation

Shi Chen [a, b, *], Yintao Zhang [c, d], Zhou Xie [c], Xingguo Song [a, b], Xinxin Liang [a, b]

[a] National Key Laboratory of Petroleum Resources and Engineering, China University of Petroleum, Beijing 102249, China
[b] College of Geosciences, China University of Petroleum, Beijing 102249, China
[c] Research Institute of Petroleum Exploration and Development, Tarim Oilfield Company, CNPC, Korla 841000, China
[d] School of Geosciences, China University of Petroleum, East China, Qingdao 266580, China

ARTICLE INFO

Keywords:
Strike–slip faults
Thrust faults
Tazhong Uplift
Tarim Basin
Hydrocarbon accumulation

ABSTRACT

The Tazhong Uplift is an important petroliferous secondary structure unit in the Tarim Basin and has undergone multiple structural deformation. In the current study, we use 3D and 2D seismic data to investigate the nature of the fault system in the Tazhong Uplift. The deformation of the Cambrian sedimentary rocks in the Tazhong Uplift is generally neglected but noted in this study. We found that the Lower–Middle Cambrian rocks are involved in thrust faults. NE-trending weak zones acted as accommodation faults formed at the connective positions and bends of the deep thrust faults. The Middle Cambrian compressional stress stemmed from the northeastern margin of the Tarim Block, pointed SW, and caused the uprising of the Tabei Uplift. The second deformation occurred in the Late Ordovician. In this instance, the compressional stress stemmed from the SW direction of the Tazhong Uplift, which originated from the amalgamation of the Western Kunlun Terrane and Tarim Block. The main strike–slip fault surfaces and subordinate faults developed along the weak zones generated in the Middle Cambrian. The collision that occurred in the southeast part of the Tarim Block in the Middle Silurian to Middle Devonian resulted in the third deformation. The representative structures that occurred during this compressive deformation were the intensive NEE-trending thrust faults in the southeast of the Tazhong Uplift. The three stages of deformation played different and important roles in hydrocarbon accumulation. These strike–slip faults holding the high-productivity hydrocarbon wells generally experienced early-stage Cambrian deformation, had wide fracture damage zones in the Ordovician carbonate rock strata, and had weak en echelon faults in the Silurian to Middle Devonian clastic rocks.

1. Introduction

Hydrocarbon exploration indicates that strike–slip faults in the central Tarim Basin show important impacts on hydrocarbon accumulation, and hundreds of highly productive wells were drilled along the faults (Fig. 1), which have been categorized as intracratonic strike–slip faults (Deng et al., 2019). The good breakthrough of the Tahe, Shunbei, and Fuman oil fields by CNPC and Sinopec has also demonstrated that strike–slip faults are closely related to the distribution of the deeply buried Ordovician karst-type carbonate reservoirs (Lu et al., 2017). The formation process and deformation mechanism of the strike-slip faults have thus been the focus of studies in the Tarim Basin (Wu et al., 2012; Li et al., 2013; Yang et al., 2013; Han et al., 2017; Qiu et al., 2019).

The Tarim Basin experienced several tectonic movements in the Paleozoic, which controlled the formation of faults and uplift and depression patterns (Nakajima et al., 1990; Jia, 1997). After the generation of a crystalline basement in the Archaeozoic and Proterozoic, the Tarim Block formed during the breakup of the Rodinia supercontinent, and paleo-oceans developed around the block (Mattern and Schneider, 2000; Xu et al., 2005; Zhang et al., 2009). The Tarim Basin was generally considered an extensional setting before the Early Ordovician (Li et al., 2013). The subduction of the paleo-oceans started in the Middle to Late Ordovician, and the margins of the Tarim Block translated into active continental margins. A representative tectonic event was the subduction and disappearance of the Kudi Ocean during the Late Ordovician (Wang et al., 2004; Sobel and Arnaud, 1999). Another important event was represented by intense Devonian thrusting and folding in front of the Altyn Mountain (Lin et al., 2009), which might have been generated by the closure of the Qilian Ocean (Sobel and Arnaud, 1999; Wu et al., 2017). The South Tianshan Ocean in the north of the Tarim

* Corresponding author at: National Key Laboratory of Petroleum Resources and Engineering, China University of Petroleum, Beijing 102249, China.
E-mail address: Chenshi4714@163.com (S. Chen).

https://doi.org/10.1016/j.jseaes.2024.106086
Received 23 August 2023; Received in revised form 15 February 2024; Accepted 24 February 2024
1367-9120/

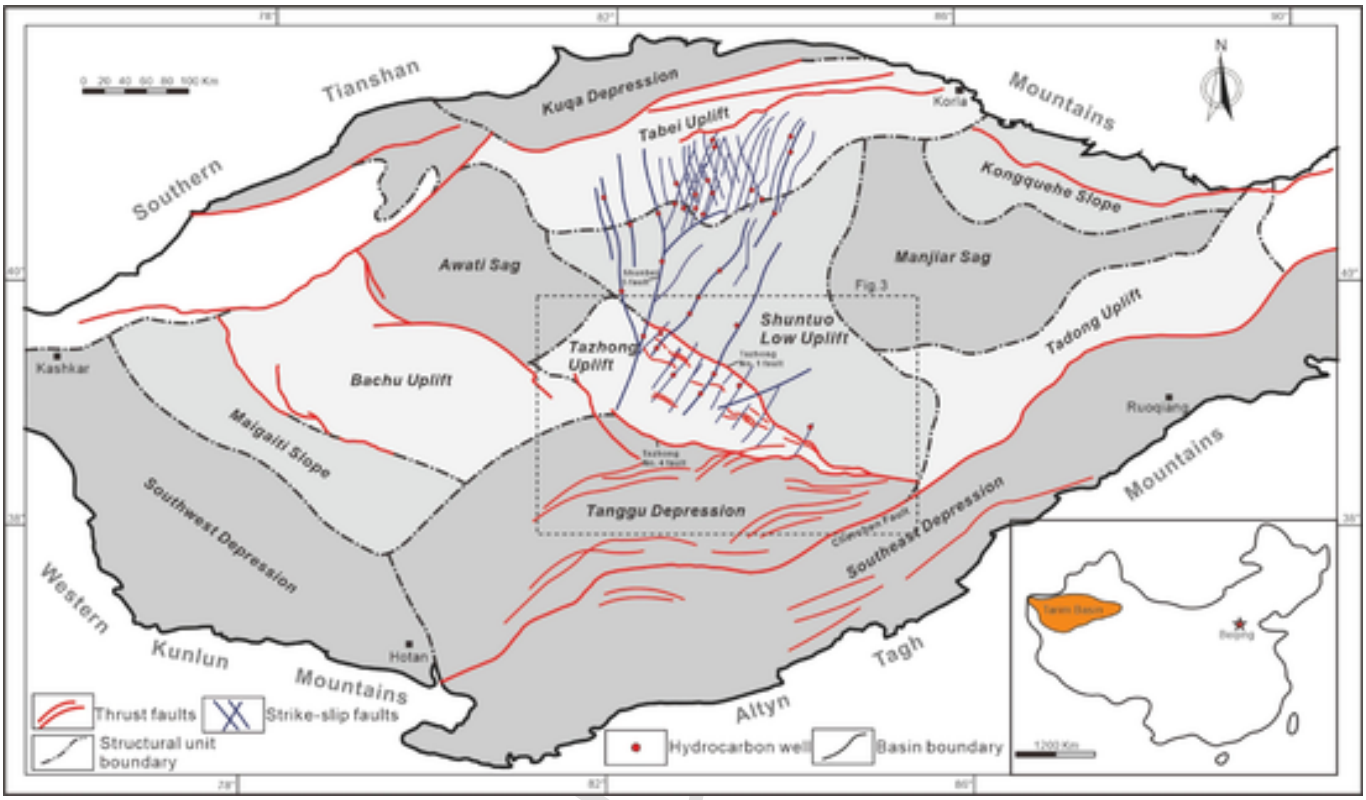

Fig. 1. Schematic diagram of the Tarim Basin showing the division of major tectonic units (the corner icon indicates the location in China).

Block was subducted and closed in a scissor-like form before the Late Carboniferous (Allan et al.,1992; Han et al., 2011). A remarkable phenomenon is the widely developed Permian magmatic activity, which might be related to a mantle plume in the Tarim Basin (Chen et al., 1997, 2006; Yang et al., 2005).

Numerous studies have investigated the structural styles, timing, and formation processes of these strike–slip faults in the central Tarim Basin. However, a great deal of debate still exists. The strike-slip faults present a conjugate style in the Tabei Uplift and have a NE-trending parallel pattern in the Shuntuo Low Uplift and Tazhong Uplift (Fig. 1). Some authors have proposed that the strike–slip faults were mainly generated during the orogenic movements around the Tarim Block in the Middle Caledonian (Zhang et al., 2011; Wu et al., 2021). By contrast, others believe that the main formation time was the Early Hercynian (Ma et al., 2012; Li et al., 2013). Recently, based on detailed structural analysis of the strike–slip faults in the Shuntuo Low Uplift, a two-stage evolution model of the Late Ordovician and Silurian to Devonian was proposed (Han et al., 2017). Detailed studies on fault segmentation, stepovers, and kinematic parameters of the strike–slip faults have also been conducted (Deng et al., 2019; Sun et al., 2021; Shen et al., 2022; Wang et al., 2022; Liu et al., 2023). However, systematic documentation of the structural evolution of fault system is still lacking. Previous studies have concentrated on the kinematic parameters and deformation processes of the strike–slip faults. Comprehensive research on fault system, deep structures, and basin basement is lacking.

The Tazhong Uplift (Fig. 1) has great petroleum potential and has undergone multiple structural deformation. The Tazhong Uplift provides an unprecedented window to research the detailed evolution of the fault system in the central Tarim Basin, due to its complicated Paleozoic strike–slip and thrust faults. In the present study, 3D and 2D seismic data from the Tazhong Uplift and surrounding areas were used to restore the complicated deformation processes of the strike–slip and thrust faults. The transformation of compressional stress in the tectonic background was analyzed, and the formation mechanism and implications for hydrocarbon accumulation in these faults were proposed. Overall, the results of the above analyses informed the proposal of an entitative relationship between strike–slip and thrust faults.

2. Geological setting and methods

The Tarim Basin is a superposed basin with a Precambrian craton basement surrounded by the Tianshan, Kunlun, and Altyn Mountains (Fig. 1), which have an area of approximately 56,000 km² in China (Li et al., 1996).

Based on the analysis of basement morphology, the development of boundary faults, and the characteristics of sedimentary covers, the Tarim Basin is generally divided into four major depressions and two major uplifts: the Kuqa Depression, Tabei Uplift, North Depression Belt, Central Uplift Belt, and Southwest and Southeast depressions from the north to the south (Fig. 1). The North Depression Belt includes the three subunits of Awati Sag, Manjiar Sag, and Shuntuo Low Uplift, whereas the Central Uplift Belt includes Bachu, Tazhong, and Tadong uplifts (Fig. 1).

The Tazhong Uplift extends in a NW–SE direction and is connected by the Bachu Uplift in its western part (Fig. 1). The Tazhong Uplift is bounded by the major Tazhong No. 1 thrust fault in the north and the southern boundary fault (Tazhong No. 4 thrust fault) in the south, which has a length of 250–300 km along the long axis and 50 km along the short axis (Fig. 1).

The Paleozoic sedimentary successions overlaying the Tazhong Uplift comprise the Cambrian to Permian system, with 22 formations. Thick beds of marine carbonate rocks developed in the Cambrian–Upper Ordovician with an evident top boundary of the Lianglitage Formation (seismic-reflecting surface of TO_{3s}) (Fig. 2). Thick gypsum and salt layers developed during the Middle Cambrian (Fig. 2). The Silurian to Permian strata are mainly composed of clastic rocks with intercalated limestone. The Permian is characterized by widespread volcanic rocks (Fig. 2).

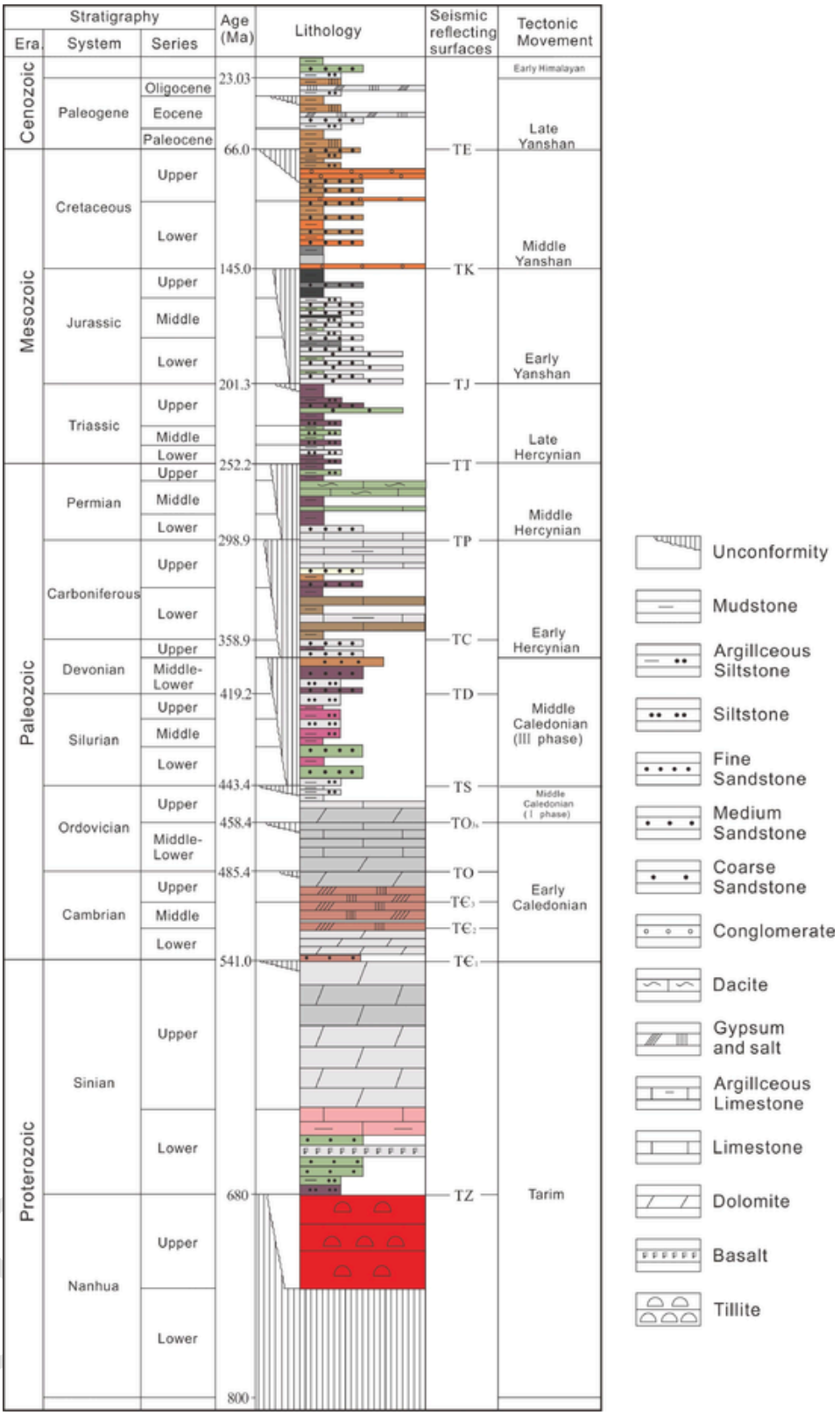

Fig. 2. Comprehensive stratigraphic column of the Tazhong Uplift showing the stratigraphy and the seismic reflecting surfaces (horizons) (obtained from Tarim Oil Company, CNPC).

The 2D and 3D seismic data were explored by Open Works (Halliburton Landmark) in this study, and the geochronologic calibration of the seismic reflectors was performed by the Institute of Exploration and Development, Tarim Oilfield Company, CNPC. Seismic coherence slices and horizontal time slices were extracted from the 3D seismic volumes. The coherence slices of interface $T\mathcal{E}_1$ (base of the Cambrian), TO_{3s} (top of the Paleozoic carbonate rocks), and TS (base of the Silurian) were utilized to investigate the structural styles, spatial distribution, and

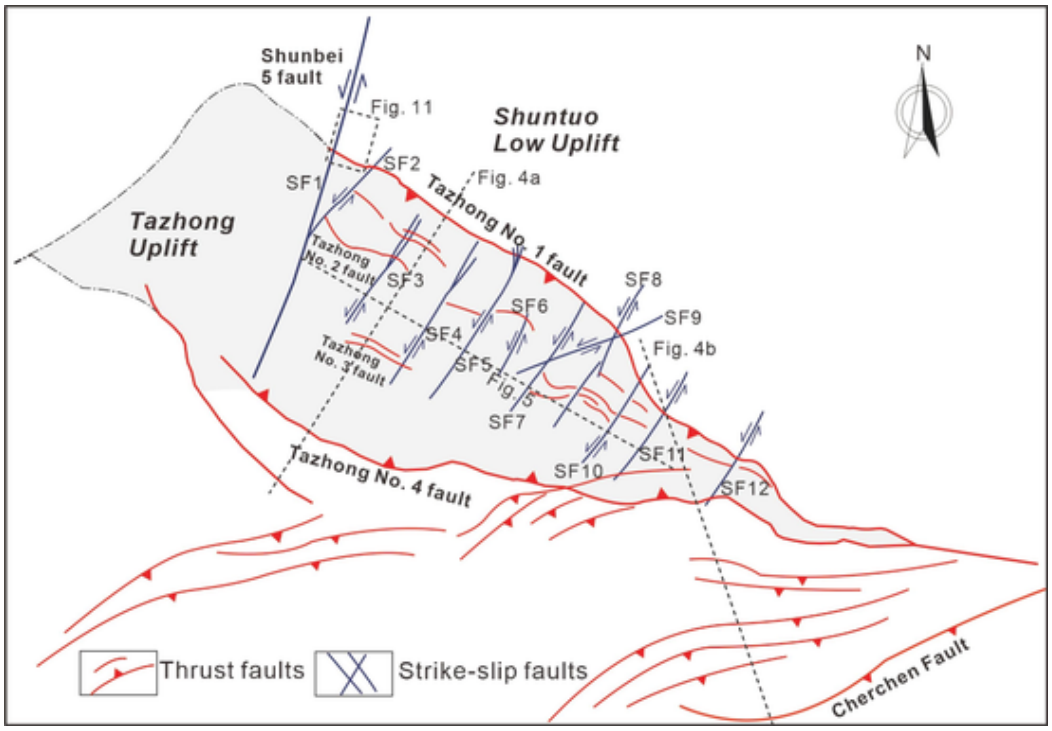

Fig. 3. Fault system diagram of the Tazhong Uplift. Three major groups of faults developed in the Tazhong Uplift and around the area: the NW-striking thrust faults, the NE-striking strike–slip faults, and a fold-and-thrust belt at the southeast end of the Tazhong Uplift. See Fig. 1b for location.

combinations of thrust and strike-slip faults. The horizontal time slices of interfaces $T\mathcal{E}_2$ (base of the Middle Cambrian) and TO_{3s} (top of the Paleozoic carbonate rocks) were produced. The time thickness maps of the Middle Cambrian and Upper Cambrian were used to analyze the change in the ancient topography.

3. Results

3.1. Overall characteristics of fault system

Three major groups of faults developed in the Tazhong Uplift and around area: the NW-striking thrust faults, the NE-striking strike–slip faults, and a fold-and-thrust belt at the southeast end of the Tazhong Uplift (Figs. 1 and 3). The NW-striking thrust faults control the morphology of the uplift and include four major faults. The Tazhong No. 1 fault is generally regarded as a boundary fault between the Tazhong Uplift and Shuntuo Low Uplift. The Tazhong No. 1 fault dips SW and extends over 160 km in a NW–SE direction. The Tazhong No. 1 fault can be further divided into three parts (Li et al., 2013). The NW-striking Tazhong No. 2 and Tazhong No. 3 fault belts each have a NE dip, and they cut the uplift (Fig. 4a). The Tazhong No. 3 fault belt represents the long axis of the Tazhong Uplift and separates it into two parts (Fig. 4a). The Southern boundary fault is generally named the Tazhong No. 4 fault belt. The Tazhong No. 4 fault belt dips to the north and extends over 200 km in a NW to nearly EW direction (Figs. 3 and 4a).

The other major fault type in the Tazhong Uplift is known as NE-striking strike–slip faults. These structures have a pervasive distribution and are perpendicular to the NW-striking thrust faults (Fig. 3). More than 10 master strike–slip faults were identified in the seismic profile (Fig. 5). These strike–slip faults generally cut and sinistrally displaced the thrust fault belts laterally (Fig. 3). Most strike–slip faults were terminated by the Tazhong No. 1 fault belt and developed horsetail splays. Individual faults cut through the Tazhong No. 1 fault and extended it into the Shuntuo Low Uplift (Figs. 1 and 3).

The third group is a fold-and-thrust belt developed at the southeast end of the Tazhong Uplift (Figs. 1 and 3). Structures in this belt have an arc-shaped planar feature and extend in a macroscopic, slightly E–W direction (Figs. 1 and 3). The thrust faults in the Tazhong Uplift were cut and modified by the arc-shaped belt at the east end of the uplift, suggesting a superimposed structure (Fig. 3). In the seismic section, the belt is characterized by basement-involved thrusts in the Tanggu Depression (Fig. 4b). The Cambrian and Ordovician strata were drawn into the thrust belt and truncated by the Carboniferous sediments, whereas the Silurian and Devonian were absent (Fig. 4b).

3.2. Thrust faults

In the NE-trending 3D seismic sections across the Tazhong Uplift, the thrust faults have an evident two-layered configuration (Fig. 6a and 7). Deep thrust faults have developed in the structural layer, which is composed of Cambrian and Precambrian strata. The deep thrust faults generally dip steeply to the NE and terminate at the base of the Upper Cambrian. Small fault-propagation folds developed in the hanging wall, and unconformities were generated at the base of the Upper Cambrian (Fig. 7). In the 3D coherency horizon slice map of the base of the Cambrian, these deep thrust faults are bow-shaped and extend subparallel in a NW–SE direction. In the western part of the Tazhong Uplift, a series of overthrust nappes were composed of several short faults, whereas the deformation was concentrated on a single fault in the eastern part of the uplift (Fig. 6a).

The superficial thrust faults are represented by belts Tazhong No. 1, No. 2, No. 3, and No. 4 (Fig. 7). Some of the faults are basement-involved thrusts, such as the Tazhong No. 3 fault, which is also characterized by steep master and back faults. The faults propagate upward from the basement, cut the Cambrian, Ordovician, Silurian, and Carboniferous strata, and were covered by the Permian. Tight folds were clamped by the master and back faults and deformed pre-Permian strata (Fig. 7b and 7e). Another type of thrust fault generally has gentle dip angles and slips off in the gypsum and salt layers within the Middle Cambrian strata, which are represented by the Tazhong No. 2 fault (Fig. 7). Gentle fault-propagation folds developed in the hanging walls, which generated a significant unconformity at the base of the Silurian

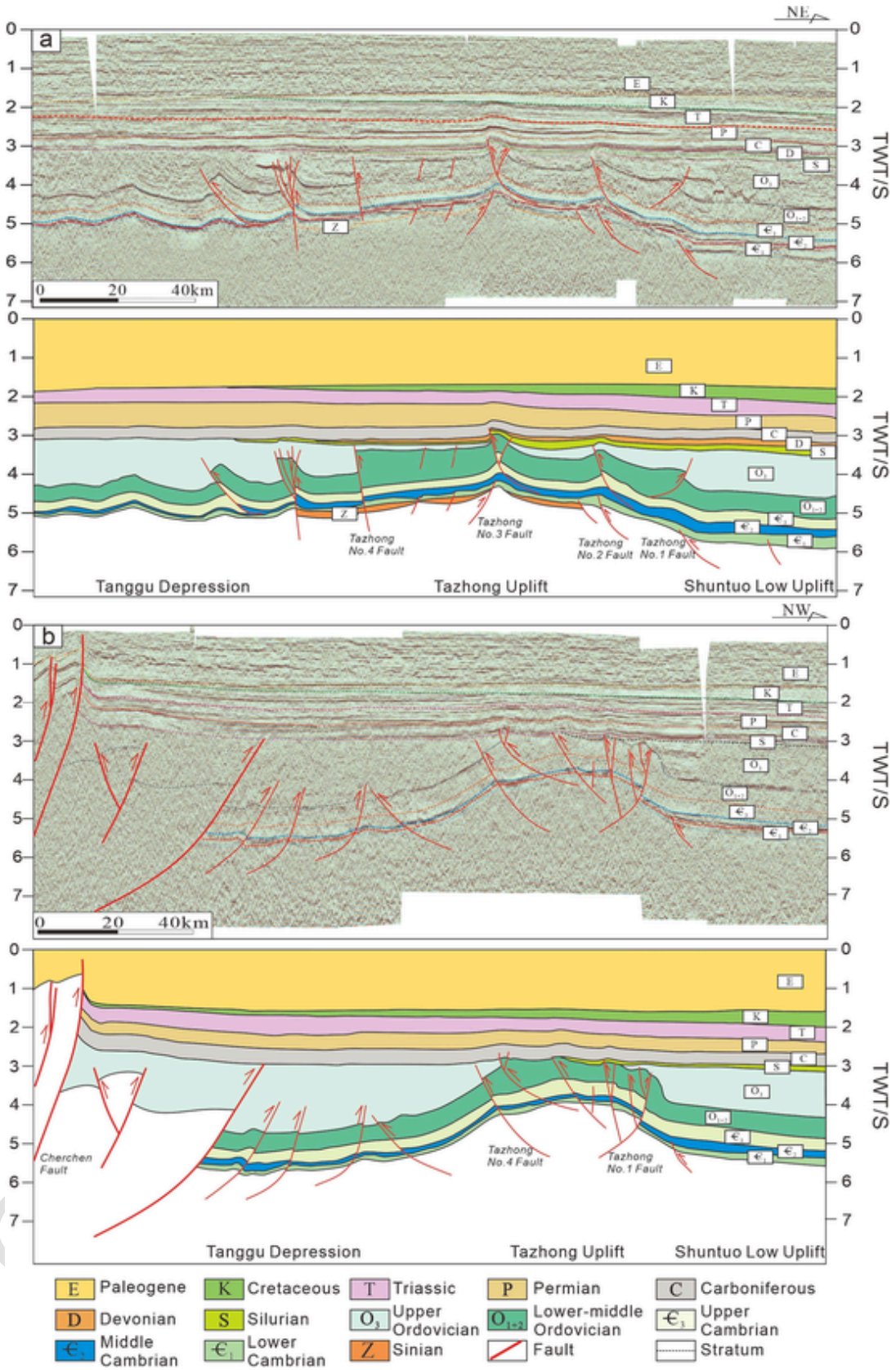

Fig. 4. Interpreted seismic profiles across the Tazhong Uplift. (a) The south-dipping Tazhong No. 1 and north-dipping Tazhong No. 4 faults constituted a large back-thrust structure that controlled the overall shape of the Tazhong Uplift. The Tazhong No. 2 and Tazhong No. 3 fault belts each have a NE dip, and they cut

Fig. 4.—*continued*
the uplift; (b) The fold-and-thrust belt developed at the southeast end of the Tazhong Uplift is characterized by basement-involved thrusts and truncated by the Carboniferous sediments. See Fig. 3 for locations.

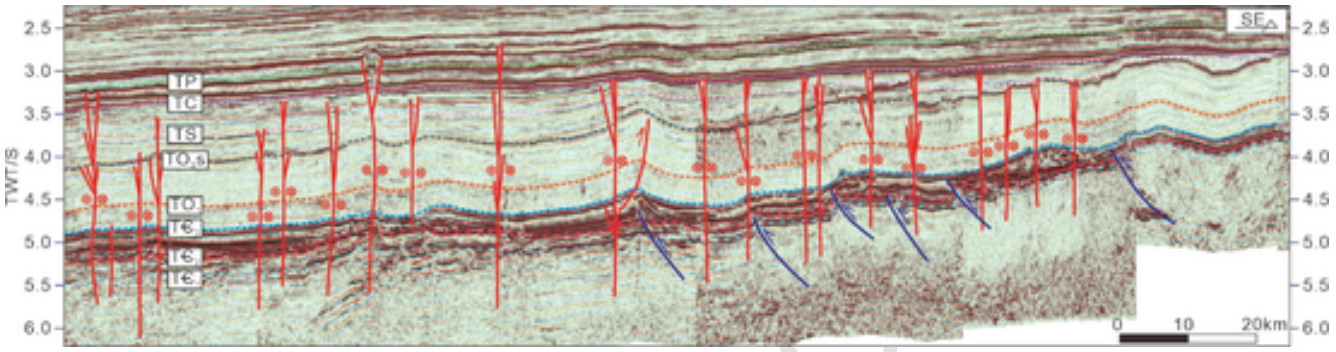

Fig. 5. Seismic profile across the Tazhong Uplift showing NE-trending strike-slip faults and stratigraphy interpretations. The strike–slip faults had a steep altitude and a recognizable flower structure. The SE part of the Tazhong Uplift was upraised, and some Devonian and Silurian deposits were eroded and truncated by Carboniferous. See Fig. 3 for location.

(Fig. 7b, 7c, 7d, and 7e). The Tazhong No. 1 fault belt configuration varies: it is basement-involved style in the west and cover decollement in the east. An asymmetric fault-propagation fold was generated on the hanging wall, with growth strata developed in the uppermost part of the Ordovician (Fig. 7a and 7c).

3.3. Strike–slip faults

In the NW-trending seismic section, the strike–slip faults had a steep altitude and recognizable flower structure (Fig. 5). However, structural analysis using the high-precision 3D seismic sections shows that the strike–slip faults have multilayer structures and present different deformation styles in different structural layers. There are five typical strike–slip faults (Fig. 8). The strike–slip faults propagate upward from the basement and are generally restricted by the Carboniferous strata, creating a composite flower structure (Fig. 8). The strike–slip faults can be divided into deep, middle, and upper structural layers in a vertical direction based on their structural characteristics.

The deep structural layer involves Lower and Middle Cambrian and Precambrian strata (Basement–T$Є_3$). In the deep structural layer, strike–slip faults generally display a nearly vertical fault surface. The offset of the phase axes along the major fault is not evident, and a small uplift and anticline controlled by the faults are evident (Fig. 8). The gypsum and salt layers suffered complicated plastic deformation due to the strike–slip faults, presenting local thickening, thinning, salt arching, and small reverse faults (Fig. 8).

The middle structural layer is composed of Upper Cambrian to Middle Ordovician carbonate rocks, Upper Ordovician mudstones, and muddy limestones (T$Є_3$–TS). In this structural layer, the vertical major and branched faults generally constitute positive flower structures. The top surface of the Lower Paleozoic carbonate rocks (TO_{3s}) exhibited a notable seismic reflection in the sections. Deformed by strike–slip faults, the surface is generally hogged to the anticline. In some cases, the hinge zones of the anticlines were cut by shallow faults, and the surface was displaced downward (Fig. 8). In the middle structural layer, the strike-slip faults generally terminate in the Upper Ordovician mudstones. These mudstones were also deformed by the faults and truncated by the base of the Silurian (TS) (Fig. 8).

The upper structural layer includes the Silurian and Devonian strata (TS–TC), which are mainly composed of clastic rocks. The strike–slip faults generally exhibit negative flower structures in this structural layer. In the seismic sections, two or more steep normal faults clamping a graben converged at depth from the negative flower structures. These shallow faults generally cut the Silurian (TS) and stopped in the Upper Ordovician, which present a composite flower structure (Fig. 8). In some cases, the shallow faults propagate downward and cut the top surface of TO_{3s}, which destroys the deep anticlines and positive flower structures (Fig. 8).

The strike–slip faults also displayed different distribution patterns at different interfaces. Based on a detailed seismic interpretation, three interfaces were selected to present the characteristics of the faults (Fig. 6): the base of the Cambrian ($TЄ_1$), the top of the Lower Paleozoic carbonate rocks (TO_{3s}), and the base of the Silurian (TS).

The strike–slip faults are intermittent at the coherence slices of the $TЄ_1$ interface. Notably, strike-slip faults were generally located at the connective positions between the two thrust faults or the bends of thrust faults (Fig. 6a). The major strike–slip faults at the interface of the TO_{3s} appear as linear structures, and are continuous. Subordinate faults developed along major strike–slip faults. Some faults displayed linear structures in the south and horsetail splays in the north (e.g., SF4 and SF5) (Fig. 6b). The thrust faults were generally cut and sinistrally displaced by the strike–slip faults (e.g., SF4, SF5 and SF8) (Fig. 6b). At the TS interface, the normal faults in the upper structural layer appear in a right-stepping en echelon arrangement along deep strike–slip faults. The normal faults have large intersecting angles (~45°) with major faults and should be interpreted as T fractures, which were formed by the sinistral displacement of the NE-striking basement faults (Tondi et al., 2012) (Fig. 6c).

4. Discussion

4.1. Timing of the deformation

Three periods of tectonic deformation were identified using the structural characteristics and unconformities: the Middle Cambrian, Late Ordovician, and Middle Silurian to Middle Devonian. The first deformation occurred in the Middle Cambrian and was represented by the deep thrust faults and the unconformity at the base of the Upper Cambrian (Figs. 7 and 9). The strike–slip faults also record this deformation through small anticlines and plastic deformation of the Cambrian gypsum and salt layers (Figs. 8 and 9).

The second stage of deformation was represented by the major Tazhong No. 1 and No. 2 thrust faults (Fig. 7). A significant unconformity appeared at the base of the Silurian strata (TS), suggesting that this deformation occurred during the Late Ordovician. The growth strata also developed in the uppermost part of the Ordovician, beside the thrust faults and folds (Fig. 7a and 7c). The main strike–slip fault surfaces formed in this period and generated positive flower structures

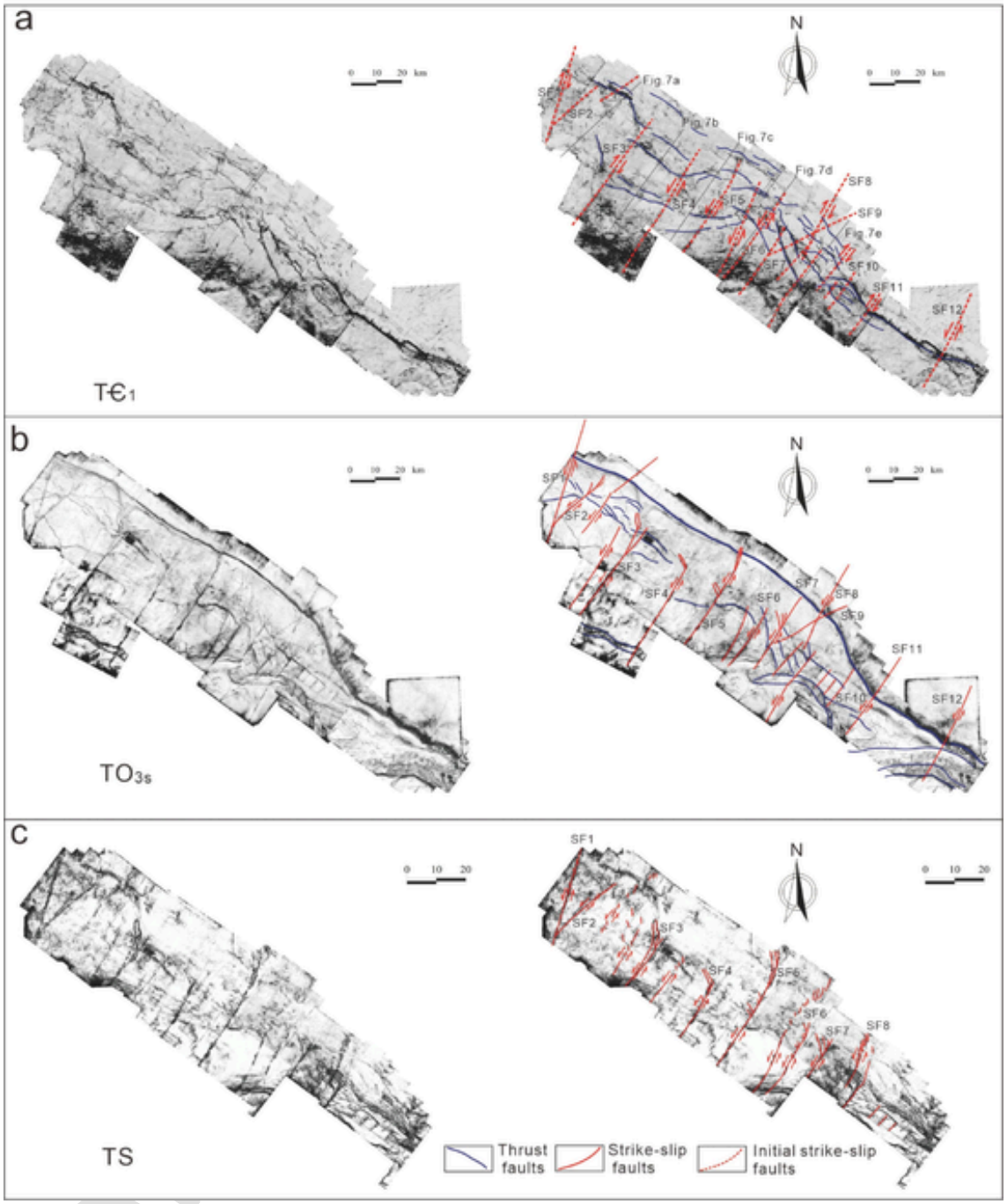

Fig. 6. 3D coherency horizon slice map of different interfaces in the Tazhong Uplift showing thrust and strike-slip fault interpretations. (a) On the $T\epsilon_1$ interface, deep thrust faults are bow-shaped and extend subparallel in a NW–SE direction. The strike–slip faults are intermittent and generally develop in the connective positions between the two thrust faults. (b) The major strike–slip faults appear as linear structures and are continuous at the interface of the TO_{3s}. Subordinate faults developed along major strike–slip faults. Some faults displayed linear structures in the south and horsetail splays in the north. (c) At the TS interface, the normal faults in the upper structural layer are in a right-stepping en echelon arrangement along deep strike-slip faults.

in the Lower Paleozoic carbonate layers (Fig. 10). Regional deformation and unconformities (Fig. 10) also developed on the top of the flower structures. Stratigraphic and structural bodies are generally terminated or displaced by fault traces on seismic slices (Nathan et al., 2014; John et al., 2015; Waldron et al., 2015). The Shunbei 5 strike–slip fault (Fig. 1) is an arc-shaped major fault that extends more than 300 km in the western part of the Shuntuo Low Uplift. In a small 3D seismic cube near the Tazhong Uplift, the offsets on the horizontal time slices of interface $T\epsilon_2$ reveal a dextral movement of the Shunbei 5 fault (Figs. 3 and 11). Meanwhile, at the interface of the TO_{3s}, the offset of the seismic events shows a sinistral movement (Fig. 11). The opposite kinematic character of the strike–slip fault also corresponds to the two-phase Middle Cambrian and Late Ordovician deformation.

The third deformation is represented by an arc-shaped fold-and-thrust belt in the Tanggu Depression that runs parallel to the Cherchen fault (Figs. 3 and 4b). The apparent unconformity before the Carboniferous constrains the deformation that occurred during the Silurian–Devonian (Fig. 4b). The NW-trending Tazhong No. 3 fault in the Tazhong Uplift also corresponds to this deformation (Fig. 7b and 7e). The en echelon-arranged normal faults along the strike–slip faults

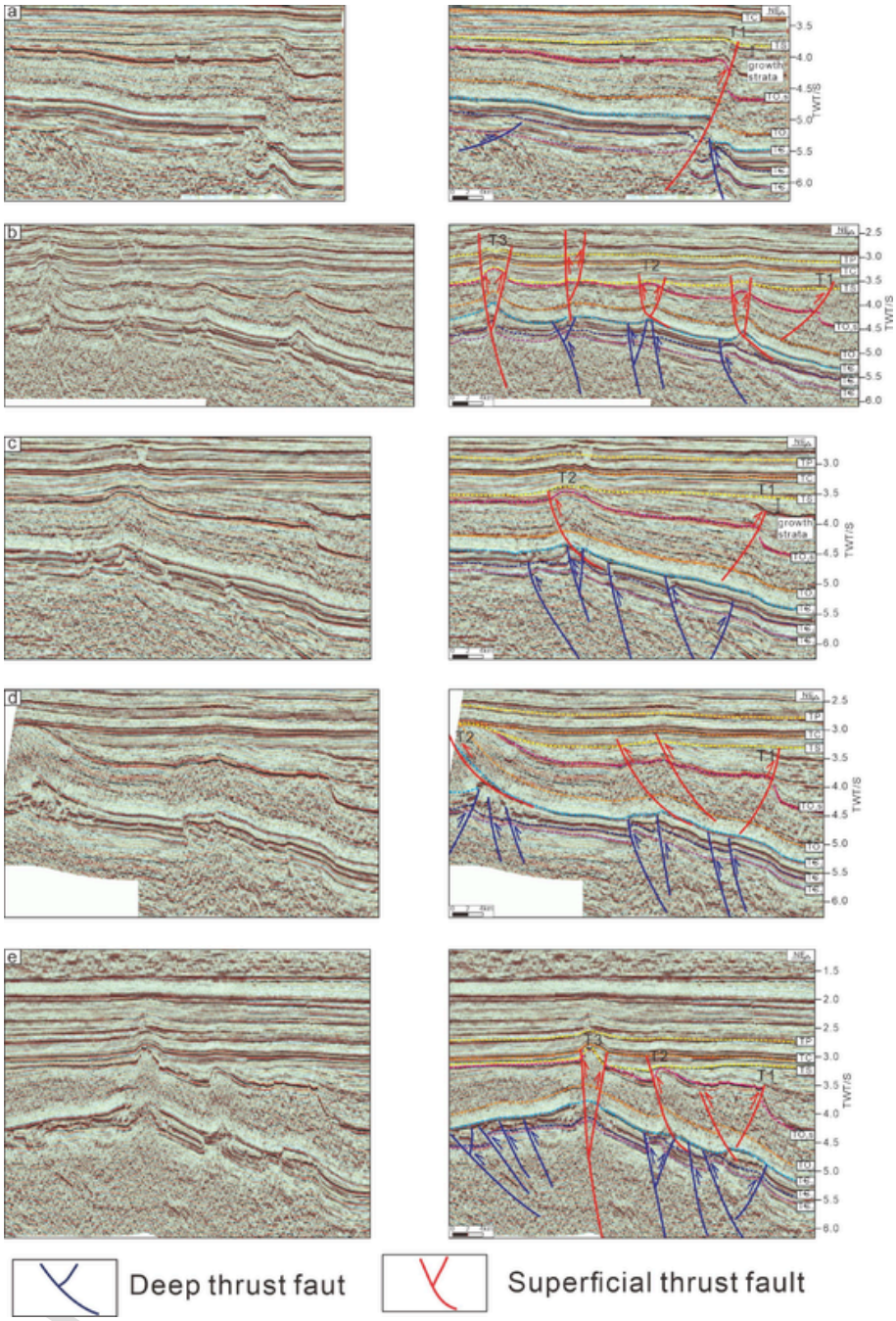

Fig. 7. Thrust faults interpreted from 3D seismic profiles in the Tazhong Uplift showing an evident two-layered configuration. The deep thrust faults generally dip steeply to the NE and terminate at the base of the Upper Cambrian, and the superficial thrust faults are represented by belts Tazhong No. 1, No. 2, No. 3, and No. 4. See Fig. 6a for locations. T1: Tazhong No. 1 fault; T2: Tazhong No. 2 fault; T3: Tazhong No. 3 fault.

formed in the Silurian–Devonian were generated during this deformation (Fig. 6c and 10). The growth index (Han et al., 2017) obtained from the growth strata controlled by shallow normal faults indicates that they were formed during the Middle Silurian to Middle Devonian (Fig. 10).

Recently, several calcite U–Pb dating ages of the cements of the strike–slip faults have been published (Wu et al., 2021; Wang et al., 2021). The ages range from the Middle Caledonian to the Late Hercynian and have several peaks of 470–430 Ma, 380–350 Ma, and 310–260 Ma (Wu et al., 2021; Wang et al., 2021). The calcite U–Pb ages thus record the latter two periods of deformation that occurred in the Late Ordovician and Middle Silurian to Middle Devonian.

4.2. Structural evolution and formation mechanism of fault system

The formation process of the strike–slip faults has been widely studied due to its control of hydrocarbon accumulation in the central Tarim Basin (Li et al., 2013; Han et al., 2017; Deng et al., 2019; Qiu et al., 2019; Sun et al., 2021; Yao et al., 2023). However, the structural timing and evolution of these faults are still highly debated. Early-phase scholars proposed that the strike–slip faults were formed during the Silurian to Devonian periods (Li et al., 2013). The scholars considered that the faults resulted from strong oblique compression from the Altyn domain during the Hercynian orogeny (Wu et al., 2011; Ma et al., 2012; Li et al., 2013). However, some authors have proposed that the NE-trending sinistral strike–slip faults acted as conjugate Riedel shear (R′) of the ma-

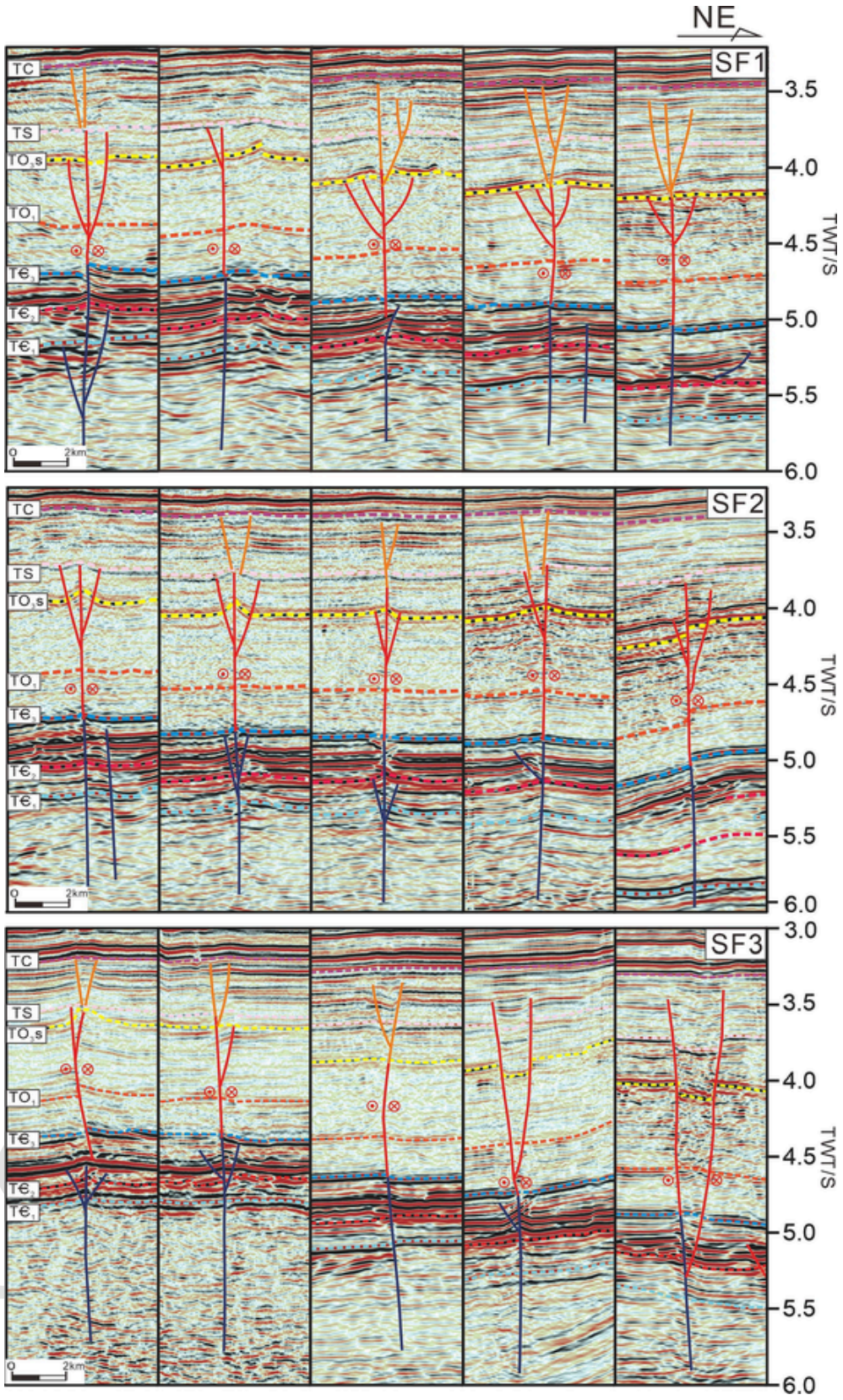

Fig. 8. Strike–slip faults interpreted from 3D seismic profile in the Tazhong Uplift. The strike–slip faults have multilayer structures and show different deformation styles in the deep, middle, and upper structural layers. See Fig. 6b for locations from SF1 to SF5.

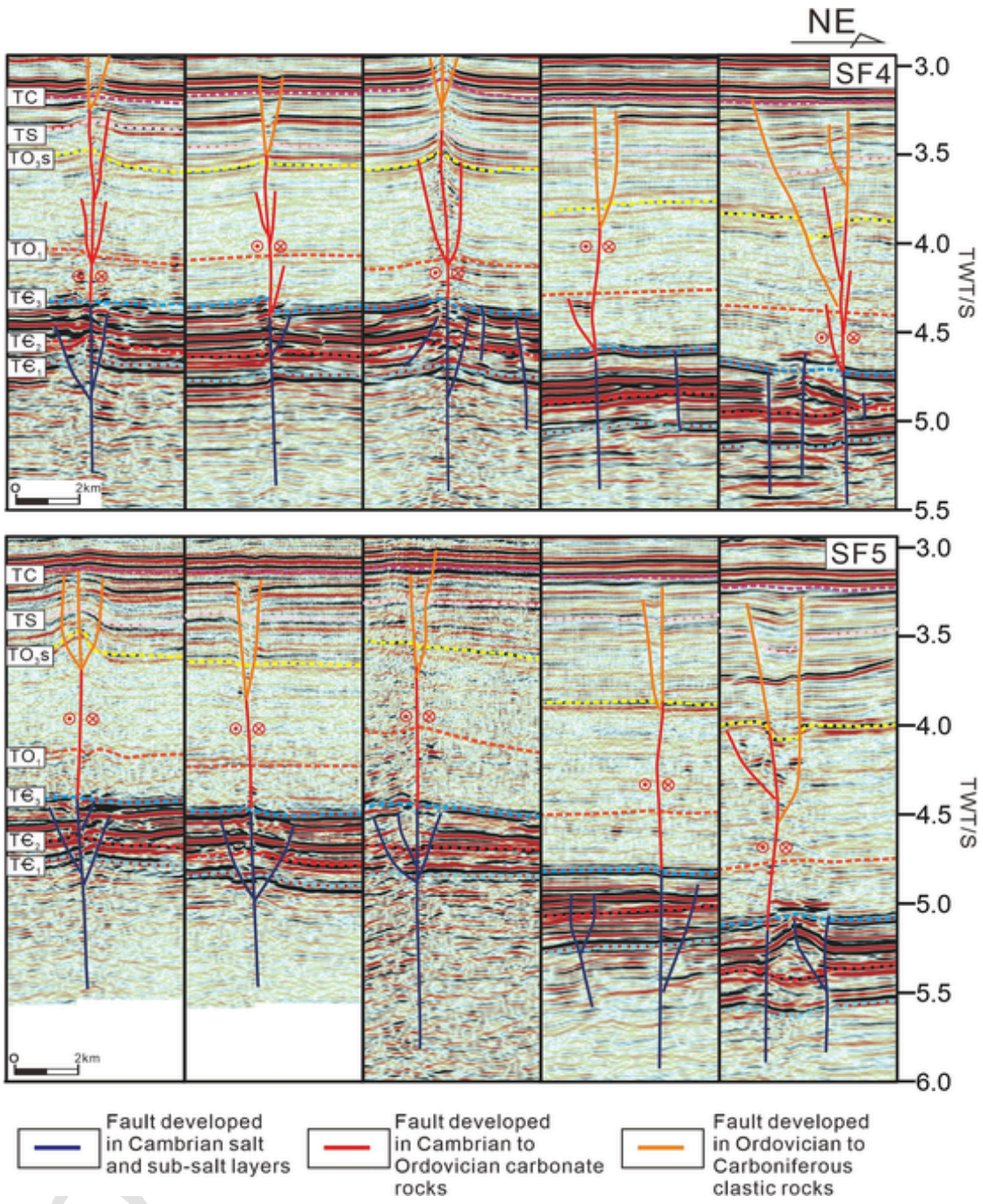

Fig. 8. (*continued*)

jor NW-striking dextral shear zone (Tazhong No. 1 and No. 4 faults) (Figs. 1 and 3), which formed during a large clockwise rotation during the Devonian (Lan et al., 2015). Recently, based on the structural analysis of the south margin of the Shuntuo Low Uplift, some authors (e.g., Han et al., 2017) have proposed that the composite flower structure of the strike–slip faults results from a two-stage deformation.

A detailed deformation process and structural evolution of the Tazhong Uplift are proposed in this study based on an integrated analysis of thrust and strike–slip faults. In the multiple tectonic evolutions of the Tarim Basin, a long-term extensional setting from the Precambrian to the Middle Ordovician has been proposed (Jia, 1997). Several key events occurred during this period. The Tarim Block was separated from the Rodinia supercontinent, and paleo-oceans developed around the block (Guo et al., 2005; Xu et al., 2013). The Kudi Ocean opened between the Tarim Block and the Western Kunlun Terrane (Mattern and Schneider, 2000). An ocean basin named the Qilian Ocean developed in the southeast of the Tarim block, separating the Qaidam, Altyn Tagh, and Eastern Kunlun terranes from the Tarim block (Yin et al., 2007). The Kudi Ocean is connected to the Qilian Ocean and forms an open ocean in the Early Paleozoic (Gehrels et al., 2003). Meanwhile, the Kunlun Ocean opened further south of the Tarim Block (Fig. 15a) (Xiao et al., 2005). The South Tianshan Ocean (Paleo-Asian Ocean) also gradually formed (Xiao et al., 2008; Han et al., 2011) (Fig. 15a).

Under the proposed long-term extensional setting (Jia, 1997), Precambrian grabens or half-grabens controlled by normal faults developed, and thick Cambrian marine deposits formed. However, a notable squeezing action occurred during the Middle Cambrian, which generated deep thrust faults in the Tazhong Uplift (Fig. 6a, 7, and 9). The

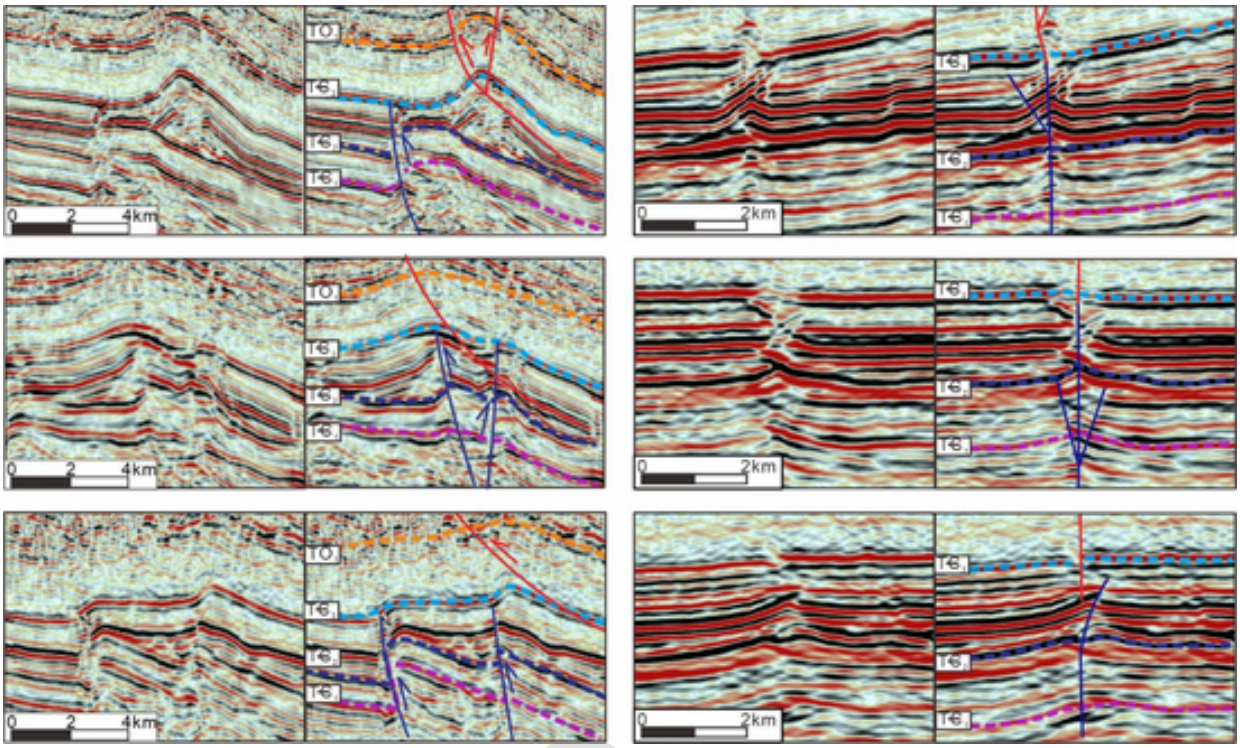

Fig. 9. Seismic profiles summarizing the Middle Cambrian deformation of the deep thrust faults and strike–slip faults. Fault-propagation folds developed in the hanging wall of the thrust faults, and unconformities were generated at the base of the Upper Cambrian. The strike–slip faults generated small anticlines and plastic deformation of the Cambrian gypsum and salt layers.

deep thrust faults generally have NE dips and a SW-bulging bow-shaped planar distribution (Fig. 6a), suggesting that the compressional stress pointed SW from the Shuntuo Low Uplift. The Middle Cambrian dextral movement of the boundary of the Shunbei 5 fault in the western Tazhong Uplift is consistent with the direction of extrusion (Fig. 11). Based on the continuous 3D seismic data, time thickness maps of Middle Cambrian (Fig. 12a) and Upper Cambrian (Fig. 12b) in the central Tarim Basin were produced, which can reflect the ancient topography at the end of the Early Cambrian (Fig. 12a) and at the end of Middle Cambrian (Fig. 12b), respectively. The center of subsidence in the Middle Cambrian was the Shuntuo Low Uplift and sedimentary grooves existed in the Tabei Uplift (Fig. 12a). At the end of the Middle Cambrian, the ancient topography changed significantly (Fig. 12b). The northeastern part of the Tabei Uplift was upraised, which caused the sag in the Shuntuo Low Uplift to extend in a NW–SE direction (Fig. 12b). In the NE-trending seismic profile, the Lower and Middle Cambrian gradually become thinner from the Shuntuo Low Uplift to the Tabei Uplift, which indicates an uplift of the Tabei area and an erosion of the Middle Cambrian (Fig. 13). Thus, the compressional stress was perpendicular to the strike of the major structural alignment (Fig. 12b). This phenomenon confirmed the Middle Cambrian deformation and the compressional stress stemmed from the northeastern margin of the Tarim Block (Fig. 12b).

It is significant that a close connection exists between thrust faults and strike–slip faults during this Cambrian squeezing action. The strike–slip faults developed at the connective positions and bends of the thrust faults, which acted as accommodation faults (tear faults) (Fig. 6a). In the horizontal time slices of interfaces of $T\epsilon_2$ of the Tazhong Uplift (Fig. 14), the kinematic characteristics of the thrust and strike–slip faults were clearly present. The strike–slip faults at the connective positions and bends of the thrust faults have opposite kinematic characters, proving the adjusted function of the strike–slip faults and the Middle Cambrian compressional stress pointed to SW and from the Shuntuo Low Uplift (Fig. 14). This phenomenon indicates that Cambrian compression generated the embryonic form of the strike–slip faults (Fig. 15a). The role of preexisting basement structures has been emphasized by previous studies, which control the development of strike–slip faults (e.g., Yang et al., 2013; Huang, 2014). However, there is no definite evidence in the geological and seismic data of basement faults. In the aeromagnetic map, NNE-striking negative and positive magnetic anomaly belts were identified in the southern area of the Tarim Block, which supports the existence of basement structures in the Tazhong Uplift (Xu et al., 2005; He et al., 2011).

The Middle Cambrian squeezing action identified in this study generated deep thrust faults and orthogonal weak zones to adjust the differential deformation, which further formed NE-trending strike–slip faults. The dynamic sources of this Cambrian deformation might be the southward subduction of the South Tianshan Ocean under the Tarim Block (Fig. 15a), coinciding with the subduction at 515–485 Ma proposed in the adjacent Junggar Ocean (Xu et al., 2012a, 2012b; Ren et al., 2014). Further investigation into the dynamics is still needed, which is beyond the scope of this study.

The Tarim Block experienced a stable continental margin and depression in the Middle to Late Ordovician. The Manjiar Sag developed during this period, in which thick Middle–Upper Ordovician carbonate sediments were deposited (Fig. 2). Significant compressive deformation occurred during the Late Ordovician, resulting in a large erosion of the Upper Ordovician on the Tazhong Uplift. The south-dipping Tazhong No. 1 and north-dipping Tazhong No. 4 faults constituted a large back-thrust structure that controlled the overall shape of the Tazhong Uplift (Fig. 4a). Growth strata developed alongside the uplift and high-angle unconformity generated at the Silurian base (Fig. 7). During this compressive deformation, the Tazhong Uplift may have been located at the leading edge of the tectonic compression and absorbed most of the shortening. The boundary Tazhong No. 1 and No. 4 faults might be preexisting weak basement zones and control the generation of the Tazhong Uplift. The compressional stress originated from the SSW direction and was perpendicular to the strike of the boundary Tazhong

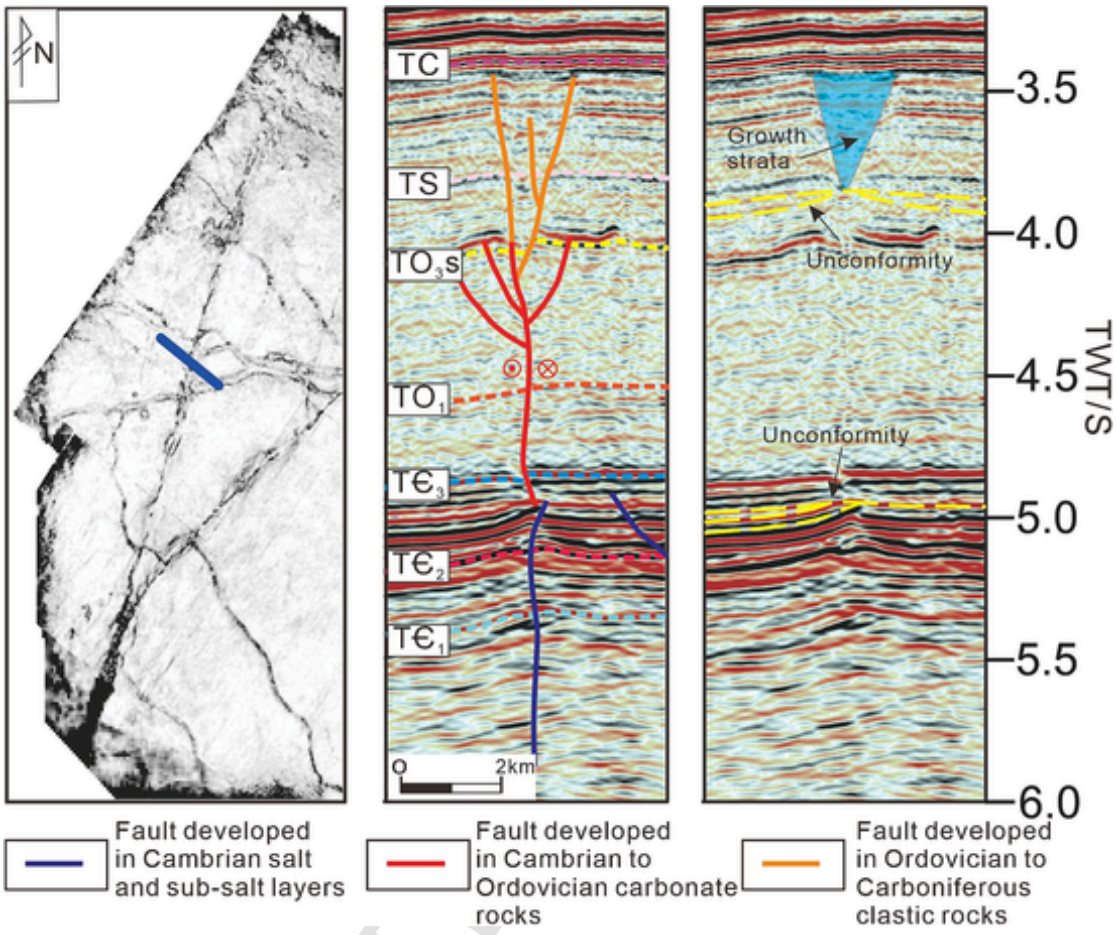

Fig. 10. Seismic profile showing three stages of deformation of the strike–slip fault. The Middle Cambrian and Late Ordovician deformation generated unconformities. The shallow en echelon-arranged normal faults controlled growth strata.

No. 1 thrust fault. Deformation concentrated in the Tazhong Uplift during this tectonic event. Under the control of the NE-striking basement weak zones formed in the Middle Cambrian, the main fault surface and subordinate faults were generated in the carbonate rock strata and constituted positive flower structures (Figs. 8 and 15b). The strike–slip faults generally have linear structures in the south and horsetail splays in the north, suggesting that the faults were restricted by the Tazhong No. 1 fault and propagated from the south to the north (Figs. 3 and 6b). The sinistral movement of the boundary of the Shunbei 5 fault in the western Tazhong Uplift also corresponds to a northward extrusion (Fig. 11). The NE-trending strike–slip faults also present sinistral displacements under the northward extrusion (Figs. 3, 6b, and 15b). These phenomena verify that the compressional stress originated from the south of the Tarim Block.

The subduction and closure of the Kudi Ocean might have occurred in the Late Ordovician, which was recorded by ~ 460 Ma arc-related granites (Sobel and Arnaud, 1999) and 453–428 Ma collision-related mylonite (Wang, 2004). This collision of the Western Kunlun Terrane should be the dynamic source of the Late Ordovician deformation in the Tazhong Uplift (Fig. 15b).

From the Silurian to the Devonian, thick clastic rocks were deposited in the Tarim Basin. Intense compression and thrusting occurred during the Devonian period. The representative structures that occurred during this compressive deformation were the intensive thrust fault system at the southeastern end of the Tazhong Uplift (Figs. 1, 3, and 4b). These faults have NEE strikes and are parallel to the structural alignment of Altyn Mountain (Fig. 1). In seismic sections, these faults generally dip steeply to the SE. The pre-Carboniferous strata were highly deformed and generated fault-propagation folds. The Devonian, Silurian, and some Upper Ordovician deposits were eroded and truncated by the base of the Carboniferous (Fig. 4b).

All the structural characteristics indicate that deformation occurred in the Devonian, and the compressional stress originated from the Altyn Mountain at the SE edge of the Tarim Block. The subduction-related high-pressure metamorphic rocks record a southward subduction of the Qilian Ocean, dated at 435 ± 20 Ma (Sobel and Arnaud, 1999). The metamorphic rocks and suture zone were intruded by Middle Devonian A-type granites, suggesting that the closure of the ocean and collision in the southeastern part of the Tarim Block occurred before the Middle Devonian (Sobel and Arnaud, 1999). The Middle Devonian thrusting was also an intensive deformation in the Tarim Basin (Jia, 1997; Wu et al., 2012), which should have originated from this collision (Fig. 15c). The intensive thrust faults in front of the Altyn Mountain absorbed the most shortening, and the Tazhong Uplift experienced a remote effect during this deformation. The SE part of the Tazhong Uplift was upraised, and some Devonian and Silurian deposits were eroded (Fig. 5). During the entire tilting of the Tazhong Uplift during the Devonian, the pre-generated NE-striking strike–slip faults suffered large-angle oblique compression. Oblique compression resulted in a small sinistral displacement of the strike–slip faults and induced en echelon normal faults in the Silurian to Devonian clastic rock layers (Fig. 6c, 8, and 10). Thus, the strikes of the normal faults were parallel to the compressional stress (Fig. 15c). The growth strata controlled by shallow normal faults indicate that they were formed during the Middle Silurian to Middle Devonian (Han et al., 2017), coinciding with the thrust faults in front of the Altyn Mountain (Fig. 1b). In this deformation, the NW-striking thrust faults in the Tazhong Uplift might have generated transpressional

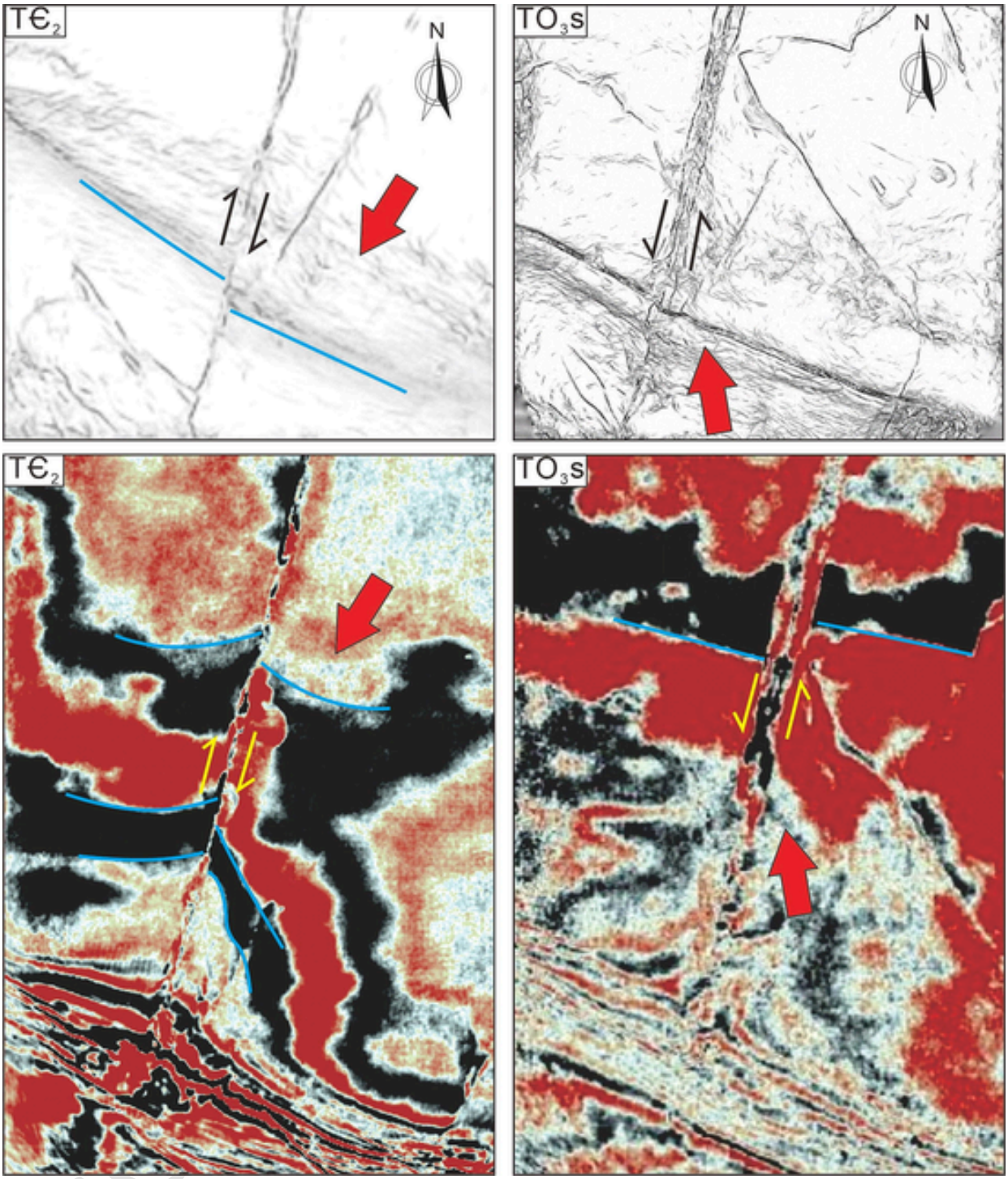

Fig. 11. Horizontal time slices of interfaces of Tϵ_2 and TO_{3s} showing opposite kinematic character of the Shunbei 5 strike–slip fault. See Fig. 3 for location.

movements, which were represented by the steep Tazhong No. 3 fault (Figs. 4 and 7).

4.3. Implications for hydrocarbon accumulation

Recent petroleum exploration suggests that strike–slip faults around the Manjiar Sag are significant for hydrocarbon accumulation in the Tarim Basin (Lu et al., 2017; Wu et al., 2020; Yang et al., 2022; Zhou et al., 2013). Hundreds of highly productive oil wells were drilled along the strike–slip faults. Several oil fields, such as the Tahe, Shunbei, and Fuman oil fields, have been constructed based on petroleum development along strike–slip faults. The producing oil strata are found in the Upper Ordovician carbonate beds in the Yijianfang and Yingshan formations (Lan et al., 2015) (Fig. 16). The solution-fracture reservoir is the most favorable reservoir type and is formed by the movements of strike–slip faults (Lu et al., 2017; Wu et al., 2020). The oil-source correlation indicates that the dark mudstones of the Lower Cambrian Yuertusi Formation are the most effective source rocks in the central Tarim Basin (Yang et al., 2022). The Yuertusi Formation is known to be the deepest source rock layer, which is covered by Middle Cambrian gypsum and salt layers (Fig. 16). The steep strike–slip faults formed the oil-source channels and connected the deep source rocks with the Ordovi-

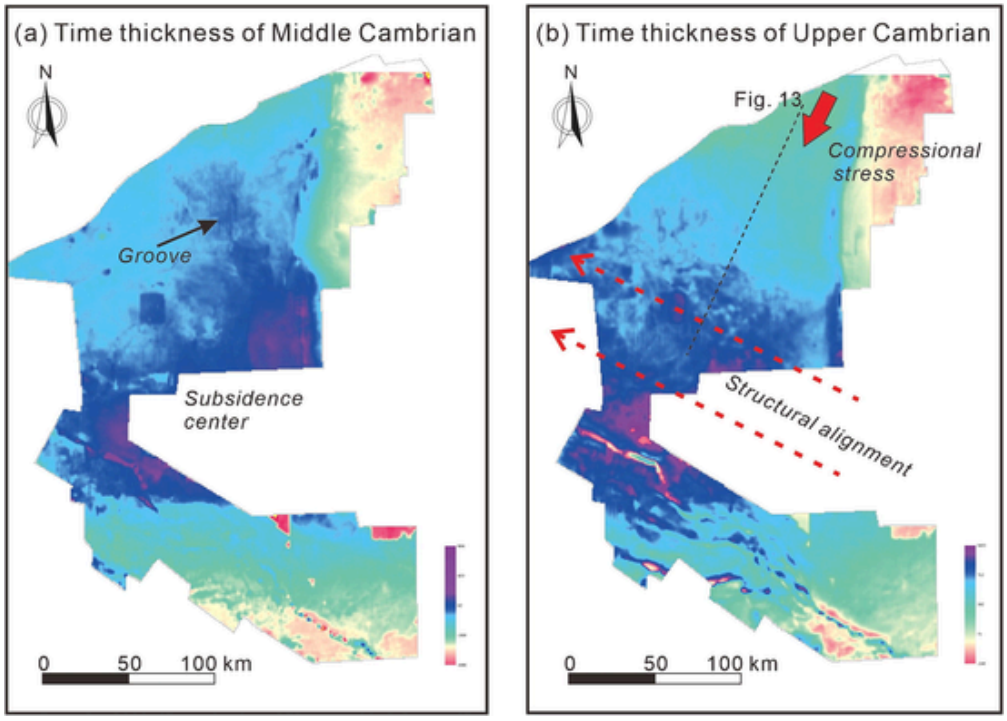

Fig. 12. Time thickness map of the Middle Cambrian (a) and Upper Cambrian (b) in the central Tarim Basin. The center of subsidence in the Middle Cambrian was the Shuntuo Low Uplift and sedimentary grooves existed in the Tabei Uplift. At the end of the Middle Cambrian, the northeastern part of the Tabei Uplift was uplifted and caused the sag in the Shuntuo Low Uplift to extend in a NW–SE direction. The compressional stress was perpendicular to the strike of the major structural alignment.

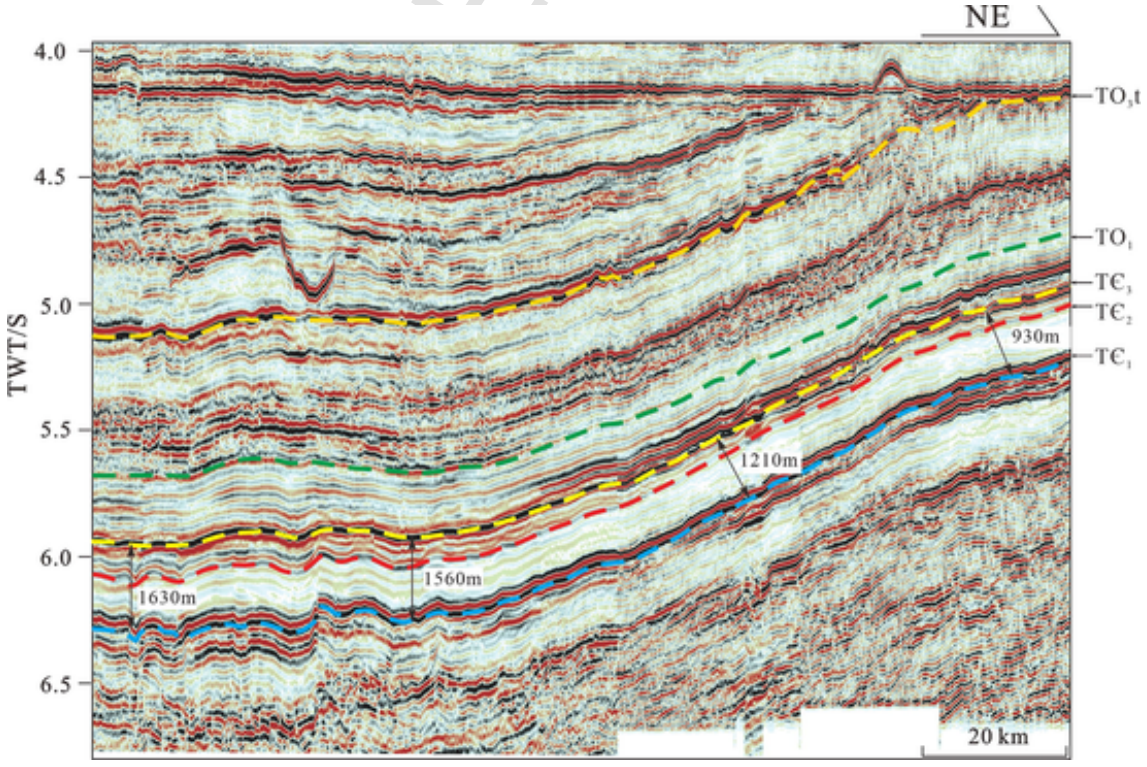

Fig. 13. NE-trending seismic profile suggesting the Lower and Middle Cambrian gradually becomes thinner from the Shuntuo Low Uplift to the Tabei Uplift.

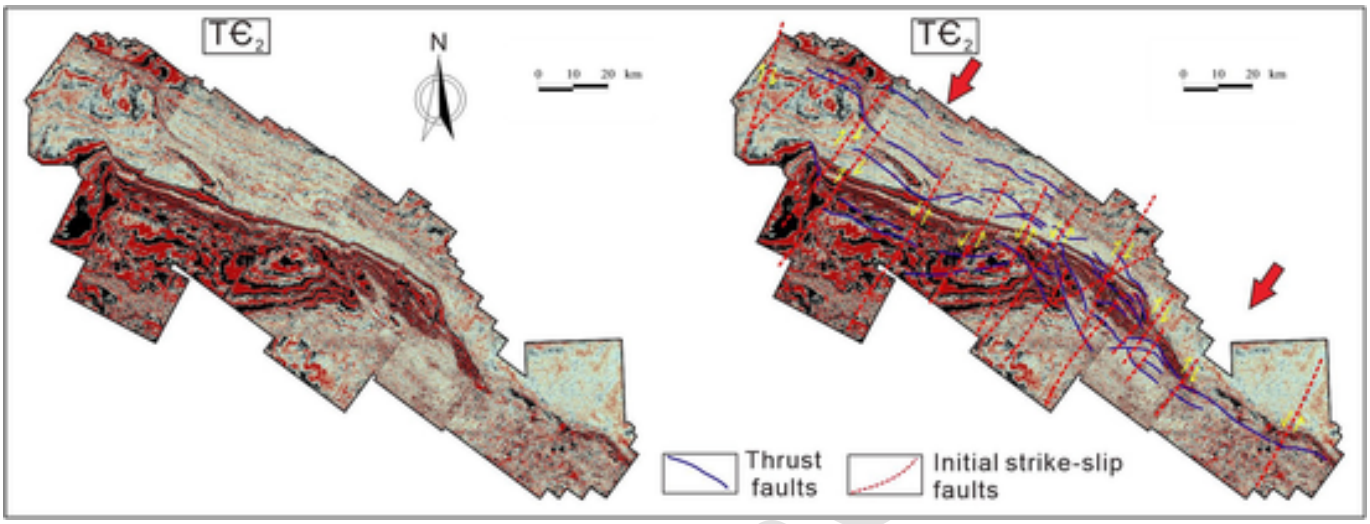

Fig. 14. Horizontal time slices of interfaces of Tϵ_2 of the Tazhong Uplift showing the kinematic characteristics of the thrust and strike–slip faults. The strike–slip faults at the connective positions and bends of the thrust faults have opposite kinematic characters.

cian carbonate rock layers in the central Tarim Basin. The strike–slip faults were both the oil-source channels and oil–gas accumulation places, which play a key role in hydrocarbon accumulation (Fig. 16).

The three stages of deformation identified in this study have played different roles in hydrocarbon accumulation on strike–slip faults. The Middle Cambrian deformation formed deep weak zones and established the foundation for the strike-slip faults. The weak zones cut through deep formations, especially the Middle Cambrian gypsum and salt layers, and created channels for hydrocarbon migration (Fig. 16). The deformation during the Late Ordovician generated the major fault surface and subordinate branches of the strike–slip faults. The faults destroyed Late Cambrian and Ordovician carbonate rocks and formed damage zones along them (Lan et al., 2015; Wu et al., 2020) (Fig. 16). The faults also formed major channels of surface water that penetrated and washed the damage zones. High-quality solution-fracture reservoirs were thus generated (Fig. 16). The strike–slip faults were covered by Silurian to Devonian clastic rocks after deformation in the Late Ordovician. The deformation in the Middle Devonian resulted in minor-scale reactivation of the strike–slip faults and the formation of shallow en echelon normal faults. The Devonian was suggested to be a major hydrocarbon expulsion stage of the Cambrian source rocks (Yang et al., 2022). Reactivation of the strike–slip faults facilitated the migration of oil and gas along the fault into the Ordovician reservoirs. However, if the shallow normal fault cuts through the Ordovician reservoirs, the oil field might be damaged, and oil and gas may leak along the faults (Fig. 16). Therefore, high-productivity wells are generally located on sections that have good oil-source channels in the deep structural layer, wide fractured zones in the middle structural layer, and weak en echelon faults in the upper structural layer. Three high-productivity wells and two failed wells were selected for a comparative study (Fig. 17). All the strike–slip faults holding the high-productivity wells experienced early-stage Cambrian deformation and had wide flower structures in the Ordovician carbonate rock. At the same time, the shallow en echelon normal faults float on top of the thick Upper Ordovician to Devonian clastic rock strata (Fig. 17). Meanwhile, the section where the failed wells were located showed weak deformation in the deep structural layer, and the shallow normal fault cut through the Ordovician reservoirs (Fig. 17).

5. Conclusions

Three stages of tectonic deformation in the Paleozoic were identified in the Tazhong Uplift. The first deformation occurred in the Middle Cambrian, and generated compressional stress pointing to the SW from the northeastern part of the Tarim Basin. The second deformation occurred in the Late Ordovician, and originated from the collision between the Western Kunlun Terrane and the Tarim Block. This collision formed compressional stress from the SW direction of the Tazhong Uplift. The closure of the Qilian Ocean in the southeast part of the Tarim Block in the Middle Silurian to Middle Devonian resulted in the third deformation.

The thrust and strike–slip faults corresponding to multistage deformation are closely related. The Middle Cambrian deformation generated deep thrust faults in the Tazhong Uplift. Weak zones developed at the connective positions and bends of the Cambrian deep thrust faults as accommodation faults (tear faults), which further formed NE-trending strike–slip faults. Late Ordovician compression generated the NW-trending major thrust faults and major shape of the Tazhong Uplift. Under the control of the NE-striking basement weak zones that formed in the Middle Cambrian, the main strike–slip fault surface and subordinate faults were generated and constituted flower structures. The Middle Silurian to Middle Devonian compressive deformation formed intensive NEE-trending thrust faults in the southeast of the Tazhong Uplift. The Tazhong Uplift was upraised, and the pre-generated NE-striking strike–slip faults suffered a large-angle oblique compression, which caused shallow en echelon normal faults.

The three stages of deformation played different roles in hydrocarbon accumulation resulting from strike–slip faults. The Middle Cambrian faults created oil source channels for hydrocarbon migration. The Late Ordovician deformation formed damage zones in the Ordovician carbonate rocks and controlled solution-fracture reservoirs. Reactivation of the strike–slip faults in the Middle Devonian facilitated the migration of oil and gas along the fault into the Ordovician reservoirs. The strike–slip faults holding the high-productivity wells generally experienced early-stage Cambrian deformation, had wide fracture zones in the Ordovician carbonate rock strata, and exhibited weak en echelon faults in the upper structural layer.

Uncited references

Xu et al. (2005a), Xu et al. (2005b), Xu et al. (2013a), Xu et al. (2012), Xu et al. (2013b).

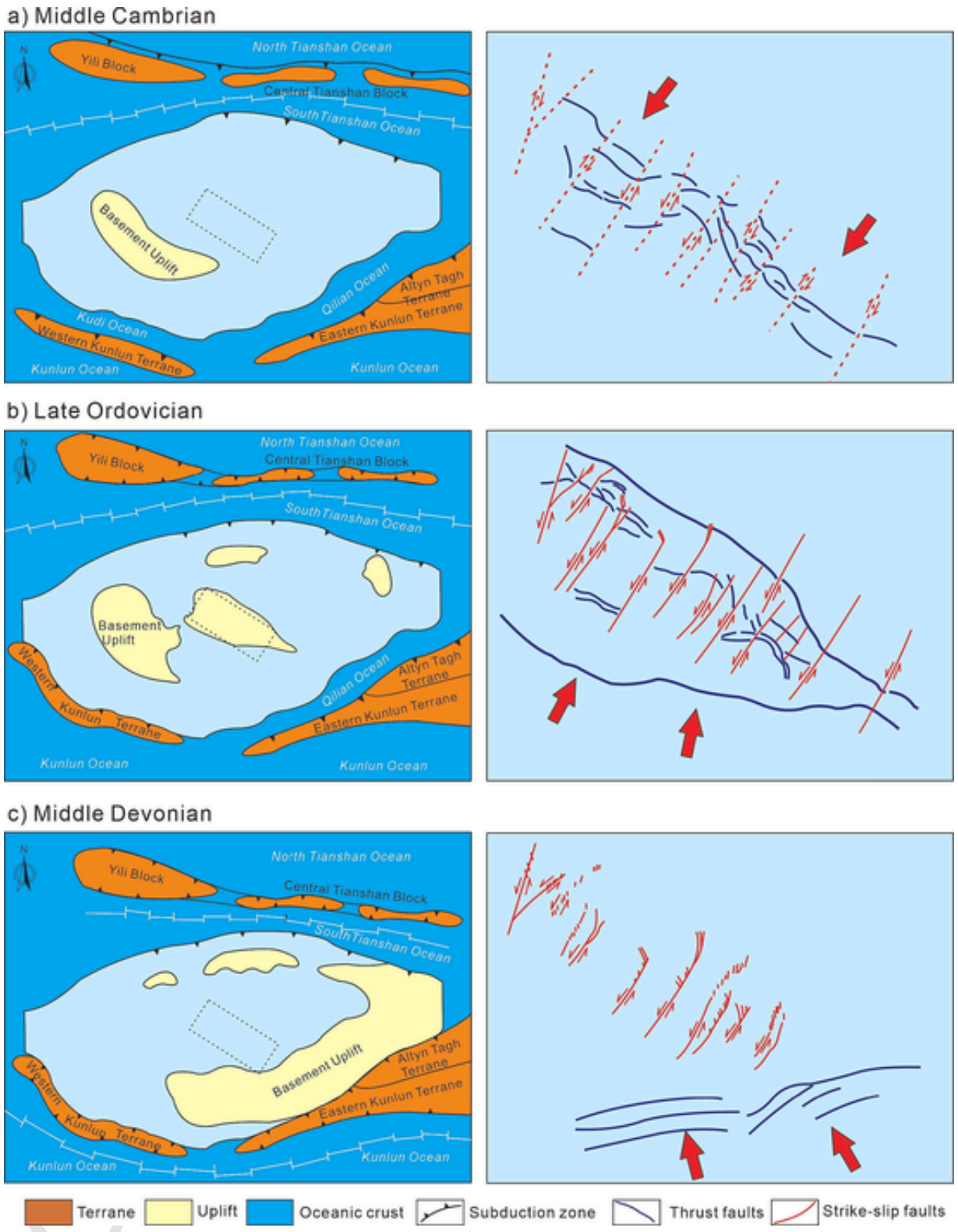

Fig. 15. Schematic geodynamic models showing the evolution of the fault system in the Tazhong Uplift. (a) Middle Cambrian: NE-trending weak zones developed at the connective positions and bends of the deep thrust faults as accommodation faults. (b) Late Ordovician: the deformation concentrated in the NW-trending thrust faults and the Tazhong Uplift was formed. Under the control of the NE-striking basement weak zones formed in the Middle Cambrian, the main fault surface and subordinate faults generated in the Paleozoic carbonate rock strata. (c) Middle Devonian: the thrust faults have NEE strikes in the SE part of the Tazhong Uplift that absorbed most shortening and the Tazhong Uplift suffered a remote effect and was upraised. The pre-generated NE-striking strike–slip faults suffered a large-angle oblique compression, resulting in a small sinistral displacement that induced the development of en echelon normal faults in the shallow clastic rock layers.

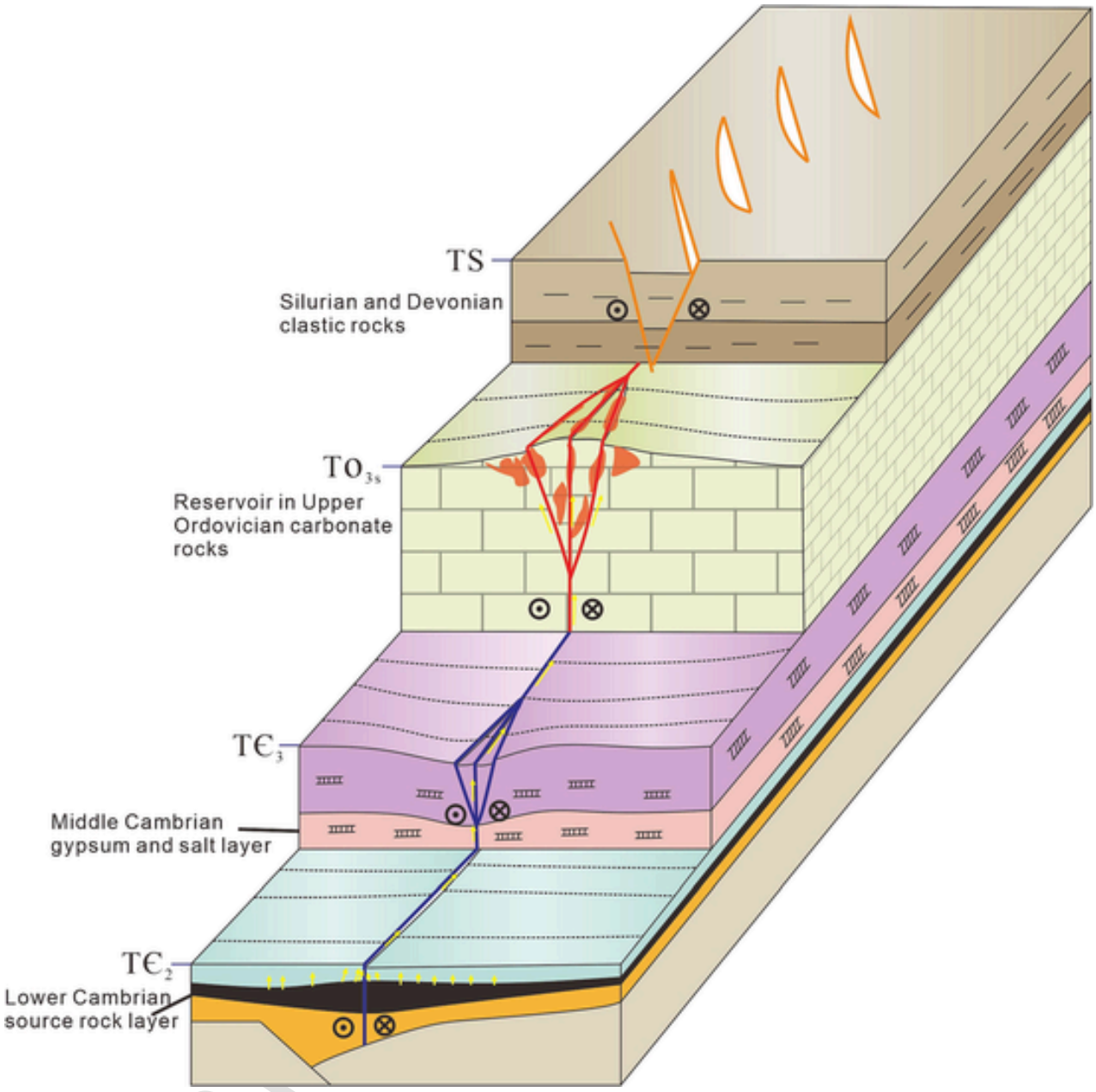

Fig. 16. Diagram of the hydrocarbon accumulation pattern by the strike–slip faults around the Manjiar Sag in the Tarim Basin.

CRediT authorship contribution statement

Shi Chen: Writing – review & editing, Writing – original draft, Methodology, Conceptualization. **Yintao Zhang:** Writing – review & editing, Supervision. **Zhou Xie:** Visualization, Investigation. **Xingguo Song:** Visualization. **Xinxin Liang:** Validation, Investigation.

Declaration of competing interest

The authors declare that they have no known competing financial interests or personal relationships that could have appeared to influence the work reported in this paper.

Data availability

Data will be made available on request.

Acknowledgements

This study was financially supported by the National Natural Sciences Foundation of China [Grant No. U21B2062].

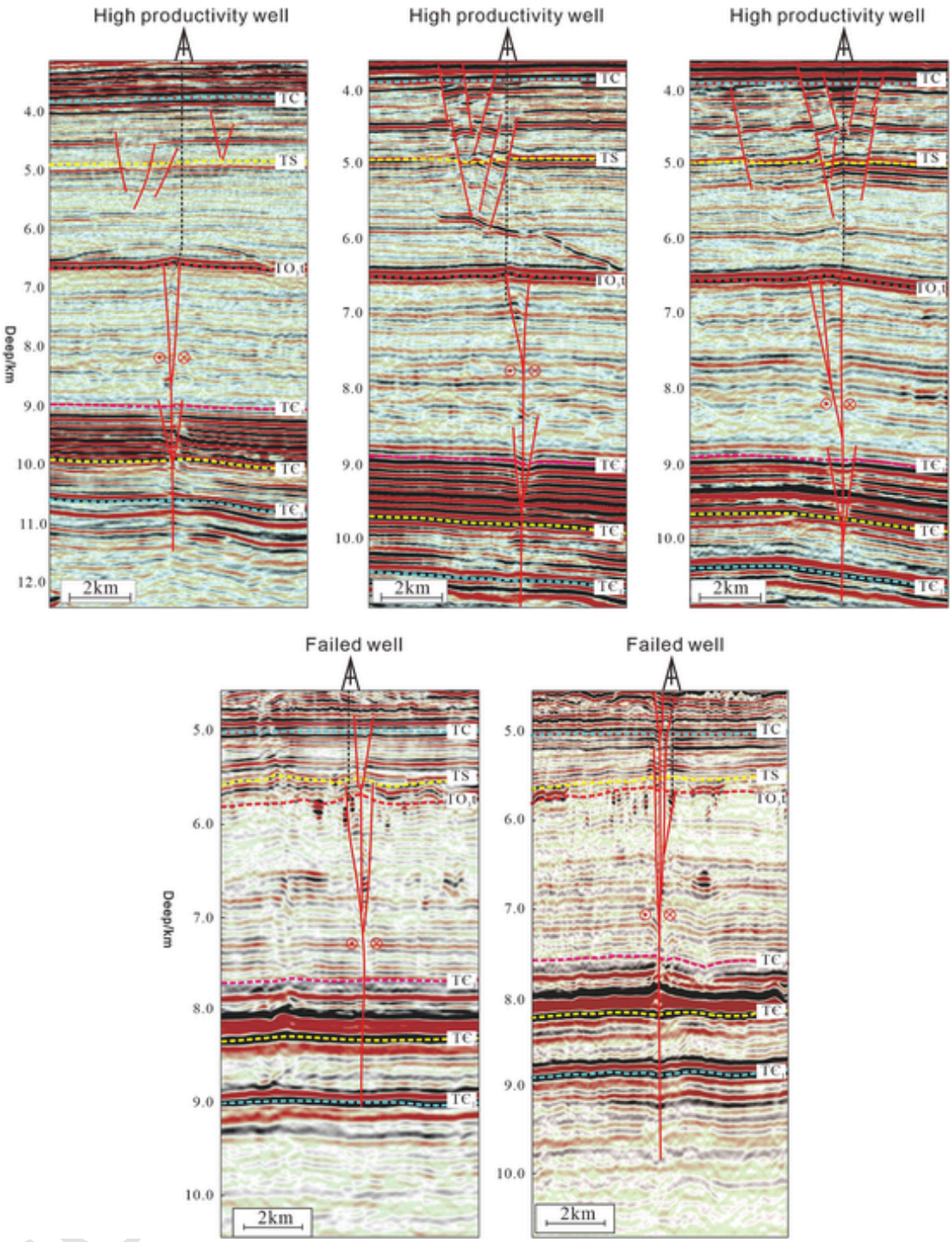

Fig. 17. Structural comparison of the high-productivity wells and failed wells. The strike–slip faults holding the high-productivity wells generally experienced early-stage Cambrian deformation, had wide fracture zones in the Ordovician carbonate rock strata, and exhibited weak en echelon faults in the upper structural layer.

References

Allan, M.B., Windley, B.F., Zang, C., 1992. Palaeozoic collisional tectonics and magmatism of the Chinese Tien Shan, Central Asia. Tectonophysics 220, 89–115.

Chen, H.L., Yang, S.F., Dong, C.W., Jia, C.Z., Wei, G.Q., Wang, Z.G., 1997. Confirmation of Permian basite zone in Tairm basin and its tectonic significance. Geochimica 26, 77–87. . in Chinese with English abstract.

Chen, H.L., Yang, S.F., Wang, Q.H., Luo, J.C., Hu, A.P., 2006. Sedimentary response to the Early-Mid Permian basaltic magmatism in the Tarim plate. Geol. China 33, 545–552. . in Chinese with English abstract.

Deng, S., Li, H., Zhang, Z., Zhang, J., Yang, X., 2019. Structural characterization of intracratonic strike-slip faults in the central Tarim Basin. AAPG Bull. 103, 109–317.

Gehrels, G.E., Yin, A., Wang, X., 2003. Magmatic history of the northeastern Tibetan Plateau. J. Geophys. Res. 108, 2423.

Guo, Z.J., Yin, A., Robinson, A., Jia, C.Z., 2005. Geochronology and geochemistry of deep-drill-core samples from the basement of the central Tarim basin. J. Asian Earth Sci. 25, 45–56.

Han, X.Y., Deng, S., Tang, L.J., Cao, Z.C., 2017. Geometry, kinematics and displacement characteristics of strike-slip faults in the northern slope of Tazhong uplift in Tarim Basin: A study based on 3D seismic data. Mar. Pet. Geol. 88, 410–427.

Han, B.F., He, G.Q., Wang, X.C., Guo, Z.J., 2011. Late Carboniferous collision between the Tarim and Kazakhstan-Yili terranes in the western segment of the South Tian Shan Orogen, Central Asia, and implications for the Northern Xinjiang, western China.

Earth Sci. Rev. 109, 74–93.
He, B.Z., Jiao, C.L., Cai, Z.H., Zhang, M., Gao, A.R., 2011. A new interpretation of the high aeromagnetic anomaly zone in central Tarim Basin. Geol. China 38, 961–969. . in Chinese with English abstract.
Huang, T., 2014. Structural interpretation and petroleum exploration targets in northern slope of middle Tarim Basin. Pet. Geol. Exp. 36, 257–267. . in Chinese with English abstract.
Jia, C.Z., 1997. Tectonic characteristics and petroleum, tarim basin, China. Pet. Ind. Press, Beijing. pp. 1-110 in Chinese with English abstract.
Lan, X.D., Lv, X.X., Zhu, Y.M., Yu, H.F., 2015. The geometry and origin of strike-slip faults cutting the Tazhong low rise megaanticline (central uplift, Tarim Basin, China) and their control on hydrocarbon distribution in carbonate reservoirs. J. Nat. Gas Sci. Eng. 22, 633–645.
Li, D.S., Liang, D.G., Jia, C.Z., Wang, G., Wu, Q.Z., 1996. Hydrocarbon accumulations in the Tarim Basin, China. AAPG Bull. 80, 1587–1603.
Li, C.X., Wang, X.F., Li, B.L., He, D.F., 2013. Paleozoic fault systems of the Tazhong Uplift, Tarim Basin, China. Marine Petrol. Geol. 39, 48–58.
Lin, C.S., Yang, H.J., Liu, J.Y., Li, P., Cai, Z.Z., Yang, X.F., Yang, Y.H., 2009. Paleostructural geomorphology of the Paleozoic central uplift belt and its constraint on the development of depositional facies in the Tarim Basin. Sci. China (Series D Earth Sciences) 52, 823–834.
Liu, Y., Suppe, J., Cao, Y.C., Hao, F., Liu, Y.D., Wang, X., Wu, K.Y., Cao, Z.C., Wei, H.H., 2023. Linkage and formation of strike-slip faults in deep basins and the implications for petroleum accumulation: A case study from the Shunbei area of the Tarim Basin, China. AAPG Bull. 107, 331–355.
Lu, X., Wang, Y., Tian, F., Li, X., Yang, D., Li, T., Lv, Y., He, X., 2017. New insights into the carbonate karstic fault system and reservoir formation in the Southern Tahe area of the Tarim Basin. Mar. Pet. Geol. 86, 587–605.
Ma, Q.Y., Sha, X.G., Li, Y.L., Zhu, X.X., Yang, S.J., Li, H.L., 2012. Characteristics of strike-slip fault and its controlling on oil in Shuntuoguole region, middle Tarim Basin. Pet. Geol. Exp. 34, 120–124. . in Chinese with English abstract.
Mattern, F., Schneider, W., 2000. Suturing of the Proto- and Paleo-Tethys oceans in the western Kunlun (Xinjiang, China). J. Asian Earth Sci. 18, 637–650.
Nakajima, T., Maruyama, S., Uchiumi, S., Liou, J.G., Wang, X., Xiao, X., Graham, S.A., 1990. Evidence for late Proterozoic subduction from 700-Myr-old blueschists in China. Nature 346, 263–265.
Nathan, B.P., Andreas, P., John, S.H., 2014. Geometry, kinematics, and displacement characteristics of tear-fault systems: An example from the deep-water Niger Delta. AAPG Bull. 98, 465–482.
Qiu, H.B., Deng, S., Cao, Z.C., Yin, T., Zhang, Z.P., 2019. The evolution of the complex anticlinal belt with crosscutting strike-slip faults in the Central Tarim Basin, NW China. Tectonics 38, 2087–2113.
Ren, R., Han, B., Xu, Z., Zhou, Y., Liu, B., Zhang, L., Chen, J., Su, L., Li, J., Li, X., Li, Q., 2014. When did the subduction first initiate in the southern Paleo-Asian Ocean: New constraints from a Cambrian intra-oceanic arc system in West Junggar, NW China. Earth Planet. Sci. Lett. 388, 222–236.
Shen, Z.Y., Neng, Y., Han, J., Huang, C., Zhu, X.X., Chen, P., Li, Q.Q., 2022. Structural styles and linkage evolution in the middle segment of a strike-slip fault: A case from the Tarim Basin, NW China. J. Struct. Geol. 157, 104558.
Sobel, E.R., Arnaud, N., 1999. A possible middle Paleozoic suture in the Altyn Tagh, NW China. Tectonics 18, 64–74.
Sun, Q.Q., Fan, T.L., Gao, Z.Q., Wu, J., Zhang, H.H., Jiang, Q., Liu, N., Yuan, Y.X., 2021. New insights on the geometry and kinematics of the Shunbei 5 strike-slip fault in the central Tarim Basin, China. J. Struct. Geol. 150, 104400.
Tondi, E., Cilona, A., Agosta, F., Aydin, A., Rustichelli, A., Renda, P., Giunta, G., 2012. Growth processes, dimensional parameters and scaling relationships of two conjugate sets of compactive shear bands in porous carbonate grainstones, Favignana Island, Italy. J. Struct. Geol. 37, 53–64.
Waldron, J.W.F., Barr, S.M., Park, A.F., White, C.E., Hibbard, J., 2015. Late Paleozoic strike-slip faults in Maritime Canada and their role in the reconfiguration of the northern Appalachian orogen. Tectonics 34, 1661–1684.
Wang, Z.H., 2004. Tectonic evolution of the western Kunlun orogenic belt, western China. J. Asian Earth Sci. 24, 153–161.
Wang, Z.Y., Gao, Z.Q., Fan, T.L., Zhang, H.H., Yuan, Y.X., Wei, D., Qi, L.X., Yun, L., Karubandika, G.M., 2022. Architecture of strike-slip fault zones in the central Tarim Basin and implications for their control on petroleum systems. J. Pet. Sci. Eng. 213, 110432.
Wang, B., Yang, Y., Cao, Z.C., He, S., Zhao, Y.Q., Guo, X.W., Liu, Y.L., Chen, J.X., Zhao, J.X., 2021. U-Pb Dating of Calcite Veins Developed in the Middle-Lower Ordovician Reservoirs in Tahe Oilfield and Its Petroleum Geologic Significance in Tahe Oilfield. Earth Sci. 46 (9), 3203–3216.
Wu, G.H., Cheng, L.F., Liu, Y.K., H, W., Qu, T.L., Gao, L., 2011. Strike-Slip Fault System of the Cambrian-Ordovician and Its Oil-Controlling Effect in Tarim Basin. Xinjiang Petroleum Geology. 32, 239-243 in Chinese with English abstract
Wu, G.H., Yang, H.J., Qu, T.L., Li, H.W., Li, B.L., 2012. The fault system characteristics and its controlling roles on marine carbonate hydrocarbon in the Central uplift, Tarim basin. Acta Petrol. Sin. 28, 793–805. . in Chinese with English abstract.
Wu, G.H., Zhao, K.Z., Qu, H.Z., Scarselli, N., Zhang, Y.T., Han, J.F., Xu, Y.F., 2020. Permeability distribution and scaling in multi-stages carbonate damage zones: Insight from strike-slip fault zones in the Tarim Basin, NW China. Marine Petrol. Geol. 114, 104208.
Wu, G.H., Ma, B.S., Han, J.F., Guan, B.Z., Chen, X., Yang, P., Xie, Z., 2021. Origin and growth mechanisms of strike-slip faults in the central Tarim cratonic basin, NW China. Pet. Explor. Dev. 48, 510–520. . in Chinese with English abstract.
Wu, C., Zuza, A.V., Yin, A., Liu, C., Reith, R.C., Zhang, J., Liu, W., Zhou, Z., 2017. Geochronology and geochemistry of Neoproterozoic granitoids in the central Qilian Shan of northern Tibet: Reconstructing the amalgamation processes and tectonic history of Asia. Lithosphere 9, 609–636.
Xiao, W.J., Windley, B.F., Liu, D.Y., Jian, P., Liu, C.Z., Yuan, C., Sun, M., 2005. Accretionary Tectonics of the Western Kunlun Orogen, China: A Paleozoic-Early Mesozoic, Long-Lived Active Continental Margin with Implications for the Growth of Southern Eurasia. J. Geol. 113, 687–705.
Xiao, W.J., Han, C.M., Yuan, C., Sun, M., Lin, S.F., Chen, H.L., Li, Z.L., Li, J.L., Sun, S., 2008. Middle Cambrian to Permian subduction-related accretionary orogenesis of Northern Xinjiang, NW China: Implications for the tectonic evolution of central Asia. J. Asian Earth Sci. 32, 102–117.
Xu, Z., Han, B.F., Ren, R., Zhou, Y.Z., Zhang, L., Chen, J.F., Su, L., Li, X.H., Liu, D.Y., 2012. Ultramafic–mafic mélange, island arc and post-collisional intrusions in the Mayile Mountain, West Junggar, China: Implications for Paleozoic intra-oceanic subduction–accretion process. Lithos 132, 141–161.
Xu, Z., Han, B.F., Ren, R., Zhou, Y.Z., Su, L., 2013a. Palaeozoic multiphase magmatism at Barleik Mountain, southern West Junggar, Northwest China: implications for tectonic evolution of the West Junggar. Int. Geol. Rev. 55, 633–656.
Xu, Z.Q., He, B.Z., Zhang, C.L., Zhang, J.X., Wang, Z.M., Cai, Z.H., 2013b. Tectonic framework and crustal evolution of the Precambrian basement of the Tarim Block in NW China: New geochronological evidence from deep drilling samples. Precambr. Res. 235, 150–162.
Xu, B., Jian, P., Zheng, H., Zou, H., Zhang, L., Liu, D., 2005a. U-Pb zircon geochronology and geochemistry of Neoproterozoic volcanic rocks in the Tarim Block of northwest China: implications for the breakup of Rodinia supercontinent and Neoproterozoic glaciations. Precambr. Res. 136, 107–123.
Xu, M.J., Wang, L.S., Zhong, K., Hu, D.Z., Li, H., Hu, X.Z., 2005b. Features of Gravitational and Magnetic Fields in the Tarim Basin and Basement Structure Analysis. Geol. J. China Univ. 11, 585–592.
Yang, S.F., Chen, H.L., Deng-Wu, J., Zhi-Long, L.I., Dong, C.W., Jia, C.Z., Wei, G.Q., 2005. Geological Process of Early to Middle Permian Magmatism in Tarim Basin and Its Geodynamic Significance. Geol. J. China Univ. 11, 504–511. . in Chinese with English abstract.
Yang, S.B., Liu, J., Li, H.L., Zhang, Z.P., Li, Q.Q., 2013. Characteristics of the NE-trending strike-slip fault system and its control on oil accumulation in north peri-cline area of the Tazhong paleouplift. Oil Gas Geol. 34, 797–802. . in Chinese with English abstract.
Yang, S., Wu, G.H., Zhu, Y.F., Zhang, Y.T., Zhao, X.X., Lu, Z.Y., Zhang, B.S., 2022. Key oil accumulation periods of ultra-deep fault-controlled oil reservoir in northern Tarim Basin, NW China. Petrol. Explorat. Devel. 49, 285–299. . in Chinese with English abstract.
Yao, Y.T., Zeng, L.B., Mao, Z., Han, J., Cao, D.S., Lin, B., 2023. Differential deformation of a strike-slip fault in the Paleozoic carbonate reservoirs of the Tarim Basin, China. J. Struct. Geol. 173, 104908.
Yin, A., Manning, C.E., Lovera, O., Menold, C.A., Chen, X., Gehrels, G.E., 2007. Early Paleozoic Tectonic and Thermomechanical Evolution of Ultrahigh-Pressure (UHP) Metamorphic Rocks in the Northern Tibetan Plateau, Northwest China. Int. Geol. Rev. 49, 681–716.
Zhang, C.L., Li, Z.X., Li, X.H., Ye, H.M., 2009. Neoproterozoic mafic dyke swarms at the northern margin of the Tarim Block, NW China: Age, geochemistry, petrogenesis and tectonic implications. J. Asian Earth Sci. 35, 167–179.
Zhang, Y.P., Yang, H.J., Lv, X.X., Liu, H., Han, J.F., Gao, Y.F., Yu, H.F., 2011. Strike-Slip Faults and Their Controls on Hydrocarbon Reservoir in Middle Part of Northern Slope of Tazhong Area, Tarim Basin. Xinjiang. Pet. Geol. 32, 342–344. . in Chinese with English abstract.
Zhou, X.Y., Lv, X.X., Yang, H.J., Wang, Y., Yu, H.F., Cai, J., Lan, X.D., 2013. Effects of strike-slip faults on the differential enrichment of hydrocarbons in the northern slope of Tazhong area. Acta Pet. Sin. 34, 628–637. . in Chinese with English abstract.